

THE SCALAR SECTOR OF THE ELECTROWEAK INTERACTIONS

Kenneth Lane
Department of Physics
The Ohio State University
Columbus, Ohio 43210

Summary

This is the report of the Higgs and Technicolor Subgroup of the Beyond the Standard Model Group at the DPF Summer Study. The official members of the subgroup were Charles Baltay, Estia Eichten, Peter Igo-Kemenes, and Kenneth Lane. In addition, we received wisdom on many matters from Ian Hinchliffe, Harris Kagan, Gordy Kane, Lawrence Littenberg, Martin Perl, Michael Peskin, and other members of the various collider working groups.

We review the properties of elementary Higgs mesons occurring in $SU(2) \otimes U(1)$ electroweak models with one or more Higgs doublets and of technipions expected in models in which the symmetry breaking is dynamical in origin. We discuss their couplings to ordinary matter, paying special attention to similarities and differences between couplings of elementary Higgses and technipions to specific channels. We also stress which couplings are reliably model-independent and which are not. We use these results to discuss the most likely production and detection modes of these mesons in e^+e^- , hadron-hadron and ep colliders and we show how to distinguish experimentally among the various scenarios for the scalar sector.

I. Introduction

The structure of the scalar sector of the electroweak interactions is perhaps the greatest mystery of high-energy physics. Even assuming that the gauge and fermion sectors are correctly described by the standard $SU(2) \otimes U(1)$ model of Glashow, Weinberg and Salam,¹ we are still completely ignorant of the precise mechanism by which $SU(2) \otimes U(1)$ is spontaneously broken down to electromagnetic $U(1)$. Of course, we all believe that the so-called Higgs mechanism² is responsible, that it gives masses both to electroweak gauge bosons W^\pm and Z^0 and to quarks and charged leptons. But, with only one rather indirect exception,³ we haven't a shred of experimental evidence that this is true nor, if it is, of what the Higgs sector consists and how it works dynamically. Settling these issues, we believe, is the most important task of high-energy physics experiments in this decade.⁴

Currently, there are two general and quite distinct scenarios for the Higgs sector. In the first, elementary (i.e., pointlike) scalar mesons are assigned to one or more doublets of the weak $SU(2)$ group. The electrically neutral components of these doublets are assumed to develop vacuum expectation values. Just why this happens no one knows; but, once it does, $SU(2) \otimes U(1)$ breaks to $U(1)_{EM}$ while fermions coupled to the Higgs mesons acquire mass. In the earliest discussions of $SU(2) \otimes U(1)$, it was assumed that only one Higgs doublet was present, and much of electroweak phenomenology (not to mention planning for experiments) has incorporated this assumption. In fact, there can be any number of Higgs doublets. The questions of how many there are, what are the masses of the physical scalars that survive the Higgs mechanism, what are their couplings to ordinary matter and so on can only be settled experimentally.

The second scenario goes under the general rubric of dynamical symmetry breaking, or "technicolor" for

short. This program attempts to give a dynamical explanation, in terms of new strong interactions at ~ 1 TeV, for the breakdown of $SU(2) \otimes U(1)$ ^{5,6} and the appearance of quark and lepton masses.^{7,8} Here, spinless mesons composed of technifermion-antifermion pairs play the role of the pointlike mesons of elementary Higgs models. The lightest and most accessible of these are called "technipions". While the idea of dynamical symmetry breaking is very attractive and natural, no phenomenologically acceptable technicolor model has been constructed. Thus, many important details of the scalar sector of technicolor are not settled theoretically - a failing they share with multi-doublet models of the elementary Higgs scenario. In any case, whether electroweak symmetry breaking is dynamically induced at 1 TeV or not is a question that must be answered. If the breaking is dynamical, mapping out the spectrum of technipions can determine their fundamental constituents, just as was done for the ordinary strong interactions.

Fortunately, the experiments of this decade can explore the scalar sector, distinguish between the two scenarios and, possibly, select among the various possibilities within each scenario. The purpose of this report is to spell out how the job can be done. We hope this report is useful to experimentalists, the intended audience.

In Section II we give a lightning review of the standard model with a single elementary Higgs doublet. This model has one observable scalar, H^0 . This summary of its properties and techniques for its discovery is included for completeness and as a contrast to the discussion of multi-doublet and technicolor models in Sections III and IV.

Section III is devoted to a detailed discussion and comparison of the general properties of charged and neutral Higgses and technipions. We begin with some of the motivations for going beyond the standard one-doublet model. Then we catalog the types of technipions and other technihadrons that may occur, using a toy model due to Farhi and Susskind⁹ as an example. Finally, we discuss what is known about the couplings of Higgses and technipions to ordinary matter, with special attention to the differences that will distinguish between them. We have taken extra care to emphasize which properties are model-independent, hence reliably known, and which are not and based merely on educated guesses.

The production and detection of the electroweak scalars in e^+e^- , hadron-hadron and ep colliders are discussed in Section IV. The couplings to ordinary matter tabulated in Section III are used to focus on the most promising means for discovering them and differentiating between the two scenarios. There we have touched only lightly on the important question of the character and estimates of backgrounds to various processes. We feel this can be well done only by the concerned experimentalists and the reader is referred to such discussions elsewhere in these proceedings.

Our main conclusions are these: (1) An e^+e^- collider with luminosity $\gtrsim 2 \times 10^{31}$ at toponium and the Z^0 can, with relative ease, discover most scalars existing below ~ 45 GeV in mass and resolve the elementary versus dynamical issue. Ultrahigh energy and luminosity e^+e^-

colliding linacs copiously produce all charged technipions. (2) $\bar{p}p$ and pp collider experiments can produce and detect only the limited class of technipions coupling strongly to gluons and, probably, none of the elementary Higgs mesons. However, given the time scale for completion of various machines, TEV I may well make the first discovery of a technipion - if it exists. (3) ep colliders are limited to production of heavy colored technipions which couple to a quark-lepton pair or to a gluon plus photon. Observable rates probably require $\sqrt{s} \sim 1$ TeV.

Much of what we say here is not new. This report has benefitted from a number of previous reviews, specifically those in Ref. 10 on the standard Higgs, H^0 , and charged Higgses and those in Ref. 11 on technipions. Also, as noted in the text, we have relied on various preliminary reports of the e^+e^- and hadron-hadron working groups at the Summer Study. This report largely may be viewed as a condensate of all those more detailed ones.

Finally, we should mention those other main currents of theoretical thought which we shall not cover explicitly. These include the scalar sector of "standard" grand-unified models, left-right symmetric models and supersymmetric electroweak or grand-unified models. To a large extent, the low-energy scalar sector of these models is phenomenologically similar to the elementary Higgs cases discussed here. Of course, we refer the reader to the appropriate group reports in the proceedings.

II. The Standard Model With a Single Higgs Doublet

A. Properties of H^0

The electroweak gauge group $SU(2) \otimes U(1)$ with a single complex $SU(2)$ -doublet of elementary (pointlike) Higgs mesons ϕ is sufficient to describe practically all known weak and electromagnetic phenomena. In this model, three of the four real component fields of ϕ combine with the W^+ , W^- and Z^0 as they become massive,^{1,2} leaving behind only a single neutral Higgs scalar, H^0 .¹² Because this minimal model is so simple, the elementary couplings of H^0 to ordinary matter-quarks, leptons and weak gauge bosons - are precisely known. The relevant couplings we shall need for production and decay of H^0 are those to fermions,

$$\mathcal{L}_{Hff} = -2\frac{1}{2}G_F^{\frac{1}{2}} \sum_{\text{fermions}, f} m_f \bar{\psi}_f \psi_f H^0, \quad (1)$$

where m_f is the so-called current-algebra mass of quark or lepton f , and those to electroweak bosons,

$$\mathcal{L}_{H(WW+ZZ)} = \left[g_W^2 W_\mu^+ W^{-,\mu} + \frac{1}{2}(g^2 + g'^2) \frac{1}{2} \mu_Z Z_\mu Z^\mu \right] H^0, \quad (2)$$

where $g = e/\sin\theta_w$, $(g^2 + g'^2)^{\frac{1}{2}} = 2e/\sin 2\theta_w$, $\sin^2\theta_w \cong 0.22$, and μ_W and μ_Z are the W^\pm and Z^0 masses, respectively. Note that there is no elementary coupling of H^0 to photons.

Unfortunately, the mass of H^0 is a free parameter of the model and, so, is completely unknown. Various theoretical and phenomenological arguments put the following very loose bounds on m_H :¹³

$$(15 \text{ MeV})_{\text{expt}} - (7 \text{ GeV})_{\text{theor}} \leq m_H \leq (1 \text{ TeV})_{\text{theor}}. \quad (3)$$

In discussing the production and decay of H^0 , therefore, the best one can do is use Eqs.(1) and (2), together with calculations of induced H^0 couplings to photons, etc., to give expectations of what will happen for various ranges of m_H . In this section, we shall assume

that $m_H \geq 5$ GeV.

The branching ratios for H^0 -decay are shown in Fig. 1 for $5 \text{ GeV} \leq m_H \leq 50 \text{ GeV}$ ¹⁴ (assuming $m_t = 20 \text{ GeV}$). If $m_H \cong 10 \text{ GeV}$, mixing with the 3P_0 -states of the T -system can become important.¹⁵ This gives a complicated dependence of decay modes on mass shown in Fig. 2. The

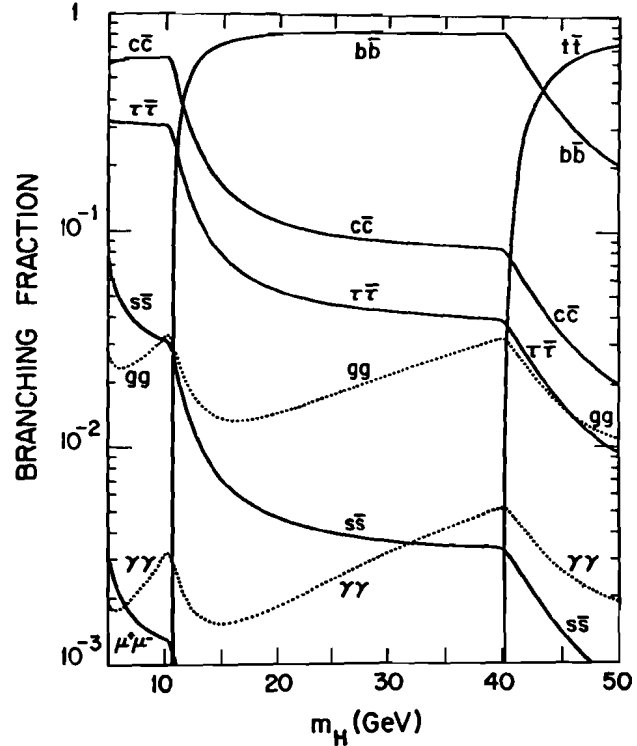


Fig. 1. Decay modes of a neutral Higgs boson with mass between 5 and 50 GeV, taken from Ref. 14.

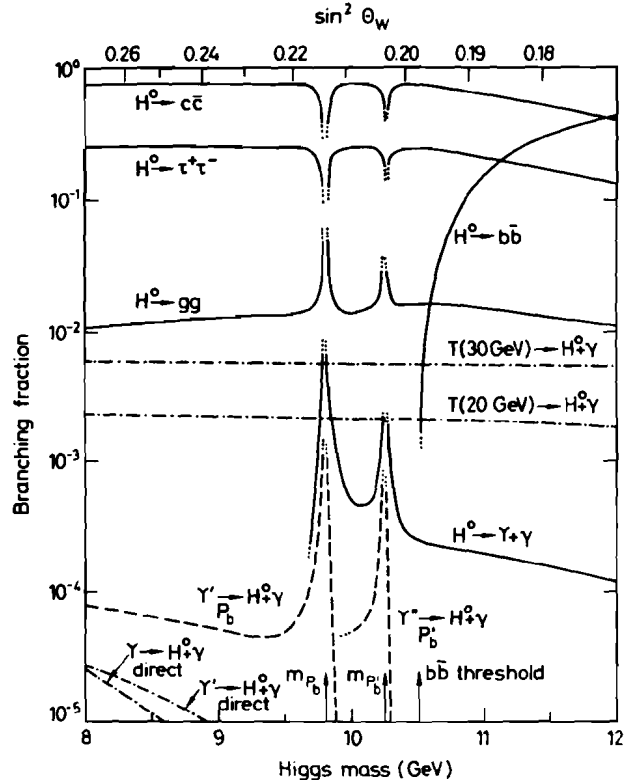


Fig. 2. Decay modes and a neutral Higgs boson with mass around 10 GeV, taken from Ref. 15.

important thing to remember is that H^0 couples to fermion mass, $\Gamma(H^0 \rightarrow \bar{f}f) \propto G_F m_f^2$, with a multiplicative factor of 3 if f is a color-triplet quark. Unless there are very heavy quarks or leptons coupling to H^0 , the modes $H^0 \rightarrow W^+W^-$ and Z^0Z^0 become dominant for $m_H > 2m_Z \approx 200$ GeV. From all this, it is clear that H^0 is best searched for by missing-mass techniques.

B. Production and Detection of H^0 in e^+e^- Colliders

1. Quarkonium $\rightarrow H^0 + \gamma$

Since H^0 couples to fermion mass (Eq.(1)), the decay rate to $H^0\gamma$ of a heavy $\bar{q}q$ 3S_1 bound state, V_q , can be appreciable. Relative to the electronic width, the rate is¹⁶

$$\frac{\Gamma(V_q \rightarrow H^0\gamma)}{\Gamma(V_q \rightarrow e^+e^-)} = \frac{G_F m_V^2}{4\sqrt{2}\pi\alpha} \left(1 - \frac{m_H^2}{m_V^2}\right), \quad (4)$$

where $m_V \approx 2m_q$. Consider toponium, $\zeta = V_t$, for example ($m_t \approx 40$ GeV). So long as $m_H \leq 0.9m_\zeta$ and there are no charged Higgses less massive than the t-quark (see Sec. III), Eq.(4) implies that $B(\zeta \rightarrow H^0\gamma) \approx 0.2\%$. With good photon detection and energy resolution ($\Delta E_\gamma/E_\gamma \approx 0.1 E_\gamma^{-1/2}$), there should be no problem reaching this limit.¹⁰ Either the H^0 can be found at toponium, or a very interesting lower bound on its mass on its mass will be set.

2. $e^+e^- \rightarrow Z^0_{\text{real}} \rightarrow H^0 Z^0_{\text{virtual}}; Z^0_{\text{virtual}} \rightarrow \ell^+\ell^-$

As can be seen from Eq.(2), there is no elementary $H^0 Z^0\gamma$ -coupling, so $e^+e^- \rightarrow Z^0_{\text{real}} \rightarrow H^0\gamma$ is not a very good way to search for H^0 . However, the relatively large $H^0 Z^0 Z^0$ -coupling makes $e^+e^- \rightarrow Z^0_{\text{real}} \rightarrow H^0 \ell^+\ell^-$ a viable way to search for H^0 .¹⁷ The rate relative to $Z^0 \rightarrow \mu^+\mu^-$ is plotted in Fig. 3¹⁸ as a function of H^0 -mass. Assuming an integrated luminosity yielding $\sim 10^7$ Z^0 /year, we see that this method is sensitive to $m_H \leq 45$ GeV (corresponding to ≈ 30 events/year). The best resolution on m_H will come from concentrating on e^+e^- pairs, for which $\Delta E_e/E_e \approx 0.1 E_e^{-1/2}$. This implies¹⁰ an acceptably small error ($\leq 25\%$) on m_H for $m_H \geq 20$ GeV. Furthermore, the backgrounds to this process, $Z^0 \rightarrow \bar{q}q \rightarrow e^+e^- \nu_e \bar{\nu}_e X$ and $e^+e^- \rightarrow e^+e^- q\bar{q}$ for example, should be relatively easy to cut away. For $m_H < 20$ GeV, $\zeta \rightarrow H^0\gamma$ probably is a better way to find H^0 . See M. Goldberg's report, and references therein, for further details.¹⁹

3. $e^+e^- \rightarrow Z^0_{\text{virtual}} \rightarrow H^0 Z^0_{\text{real}}$

Finally, if $m_H > 45$ GeV, the only resort in lepton colliders is to crank up the energy well above the Z^0 mass and again take advantage of the large $H^0 Z^0 Z^0$ -coupling. The final Z^0_{real} probably is best detected in its e^+e^- -decay mode. For $\sqrt{s} \leq 175$ GeV and $\mathcal{L} = 2 \times 10^{31}$ $\text{cm}^{-2} \text{sec}^{-1}$, this method is sensitive to Higgs masses ≤ 60 GeV.

In closing this discussion, we mention that the development and implementation of vertex detectors which can find the decay kinks of τ 's, c 's and b 's resulting from H^0 -decay can enhance substantially the probability of finding H^0 in each of these e^+e^- production mechanisms.

C. Production and Detection of H^0 in Hadron-Hadron Colliders

Discovery of the H^0 at existing or proposed pp and $\bar{p}p$ colliders will be a difficult, if not impossible, task. Three of the more promising production modes

mentioned in the literature are discussed here.

1. pp or $\bar{p}p \rightarrow H^0 + X$ via Quark Fusion; $H^0 \rightarrow \mu^+\mu^-$

Ellis, Gaillard and Nanopoulos¹⁰ proposed production of H^0 from valence and sea quarks in the nucleon and detection via the $\mu^+\mu^-$ decay mode of H^0 . They find

$$\frac{\sigma(pp \rightarrow H^0 X \rightarrow \mu^+\mu^- X)}{\sigma(pp \rightarrow \mu^+\mu^- X)} \approx 10^{-3} \frac{m_H}{\Delta m_H} \frac{\Gamma(H^0 \rightarrow \mu^+\mu^-)}{\Gamma(H^0 \rightarrow \text{All})}, \quad (5)$$

where $\Delta m_H/m_H$ is the μ -pair invariant mass resolution at the Higgs mass. $m_H/\Delta m_H$ is unlikely to be much larger than 10. The factor of 10^{-3} come from assuming an SU(3)-invariant sea and is due to the smallness of $G_F m_S^2$ ($m_S \approx 175$ MeV). Thus, Eq.(5) is a drastic overestimate for production in the case of $\bar{p}p$ collisions because the Drell-Yan cross section in the denominator is dominated by valence quark-antiquark annihilation.

From Eq.(1) and Fig. 1, it is clear that $B(H^0 \rightarrow \mu^+\mu^-) < 3 \times 10^{-4}$ (for $m_H \approx 5$ GeV), and it falls to 8×10^{-6} for $m_H > 2m_t$ assuming a 20 GeV top-quark mass. Thus, this method amounts to looking for a peak for which the signal-to-background is at most 10^{-6} .

2. H^0 From Gluon-Gluon Fusion

To avoid the suppression factor $G_F m_q^2$ in H^0 -production due to its direct coupling to light quarks, Georgi, et al., proposed a gluon-fusion mechanism.²⁰ Here, H^0 is produced through its coupling to a pair of gluons, a coupling which is not suppressed when it is induced by heavy quark loops for which $m_q \gg 0.2 m_H$. For quark masses satisfying this inequality, the quark-mass dependence

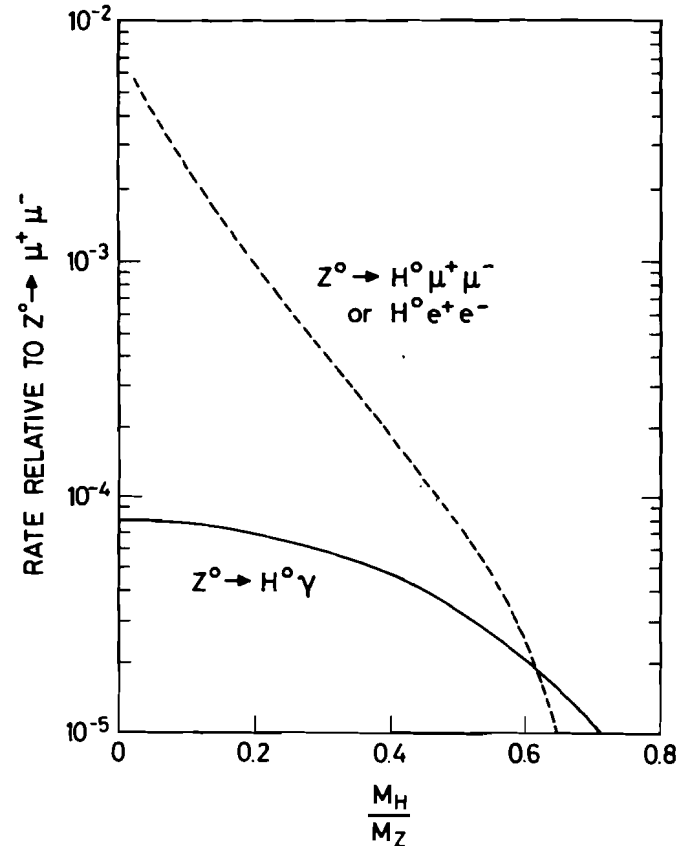


Fig. 3. Decay rates for $\Gamma(Z^0 \rightarrow H^0 + \gamma)/\Gamma(Z^0 \rightarrow \mu^+\mu^-)$ and $\Gamma(Z^0 \rightarrow H^0 + \mu^+\mu^- \text{ or } e^+e^-)/\Gamma(Z^0 \rightarrow \mu^+\mu^-)$ for different values of m_H/m_Z ; taken from Ref. 18.

drops out and the production cross section is proportional to $\alpha_s^2 G_F N_f^2$, where N_f is the number of contributing heavy quark flavors. The authors calculated the production cross section in pp collisions up to $\sqrt{s} = 400$ GeV. It is ~ 30 pb for $m_H \approx 5$ GeV, falling to 1 pb for $m_H \approx 70$ GeV. (See Fig. 4.) The problem still is: How is one to detect H^0 ? Even ignoring the difficulty of making invariant mass plots of $\tau^+\tau^-$, $c\bar{c}$, $b\bar{b}$ and so on, each of these Higgs decay modes must lie on a horrendous background. We believe this method will not work, but defer to the judgement of anyone who has given this mechanism more careful thought.

3. Associated Production of H^0 With Z^0 or W^\pm 21

This method, which relies on the relatively large $H^0 Z^0 Z^0$ and $H^0 W^+ W^-$ couplings, is the hadronic collider analog of the H^0 search in $e^+e^- \rightarrow Z^0 \rightarrow H^0 \ell^+ \ell^-$ and it seems the most promising. The $p\bar{p}$ and pp cross sections for $H^0 Z^0/H^0 W^\pm$ + anything, relative to Z^0/W^\pm + anything, are shown in Figs. 5 and 6. For the interesting mass range $m_H \geq 10$ GeV, the cross section is small and falling rapidly with increasing m_H .

For $m_H < \mu_Z$, L.-L. Chau Wang has suggested concentrating on $Z^0 \rightarrow H^0 Z^0 \rightarrow H^0 \ell^+ \ell^-$ and looking for a bump at $M_{\ell^+ \ell^-} = \mu_Z - m_H$ in the dilepton invariant mass distribution.²² For $m_H = 15$ GeV and Isabelle parameters, $\sqrt{s} = 800$ GeV and $\int \mathcal{L} dt = 10^{40} \text{ cm}^{-2}$ in 10^7 sec, she predicts an excess of ~ 200 events in the bump between 60 and 80 GeV. (The excess is ~ 1 event for TEV I parameters.) To reduce backgrounds due to $\gamma\gamma$ and Z^0 , she suggests triggering on a third, low-energy lepton resulting from semileptonic decay of Higgs decay products. From Fig. 5b, it is clear that this proposal is useful only for $m_H \leq 20$ GeV. For $20 \text{ GeV} \leq m_H \leq 2\mu_Z \approx 200$ GeV, discovery of H^0 by associated production will require detection and reconstruction of its decay products in addition to triggering on Z^0 or W^\pm . For $m_H > 200$ GeV, $H^0 \rightarrow Z^0 Z^0$ and $W^+ W^-$ are its major decay modes. Then one can attempt to trigger on two or three elec-

troweak bosons - a striking signal with a dreadfully small rate at existing and proposed colliders

To sum up: If H^0 exists and is less massive than ~ 60 GeV, it should be possible to discover it with relative ease at e^+e^- colliders, assuming LEP II energies and luminosities $\sim 2 \times 10^{31} \text{ cm}^{-2} \text{ sec}^{-1}$. We emphasize that the simplest method probably is toponium - $H^0 + \gamma$ if H^0 is light enough. By contrast, production and, especially, detection of H^0 in proposed pp and $p\bar{p}$ colliders will be very difficult.

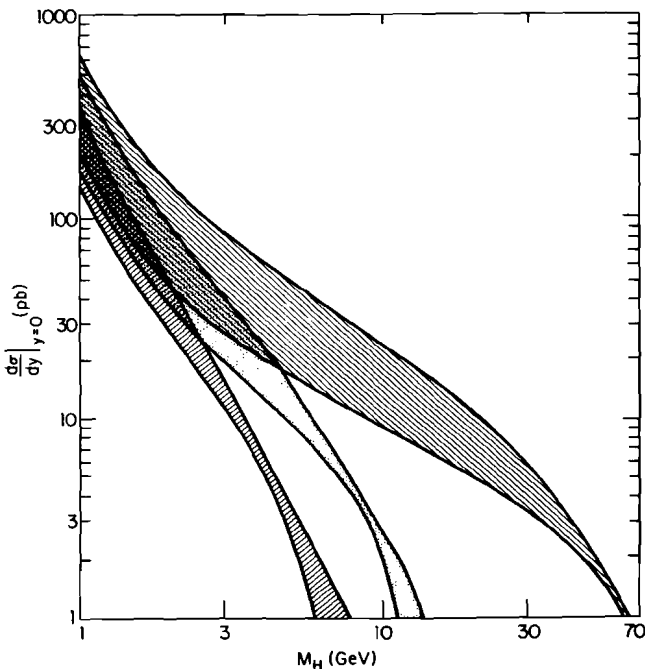


Fig. 4. $d\sigma_H/dy|_{y=0}$ as a function of H mass, taken from Ref. 20. Each shaded band represents a different center-of-mass energy; $\sqrt{s} = 27.4$ GeV (slash up to the right), $\sqrt{s} = 60$ GeV (dot), and $\sqrt{s} = 400$ GeV (slash up to the left).

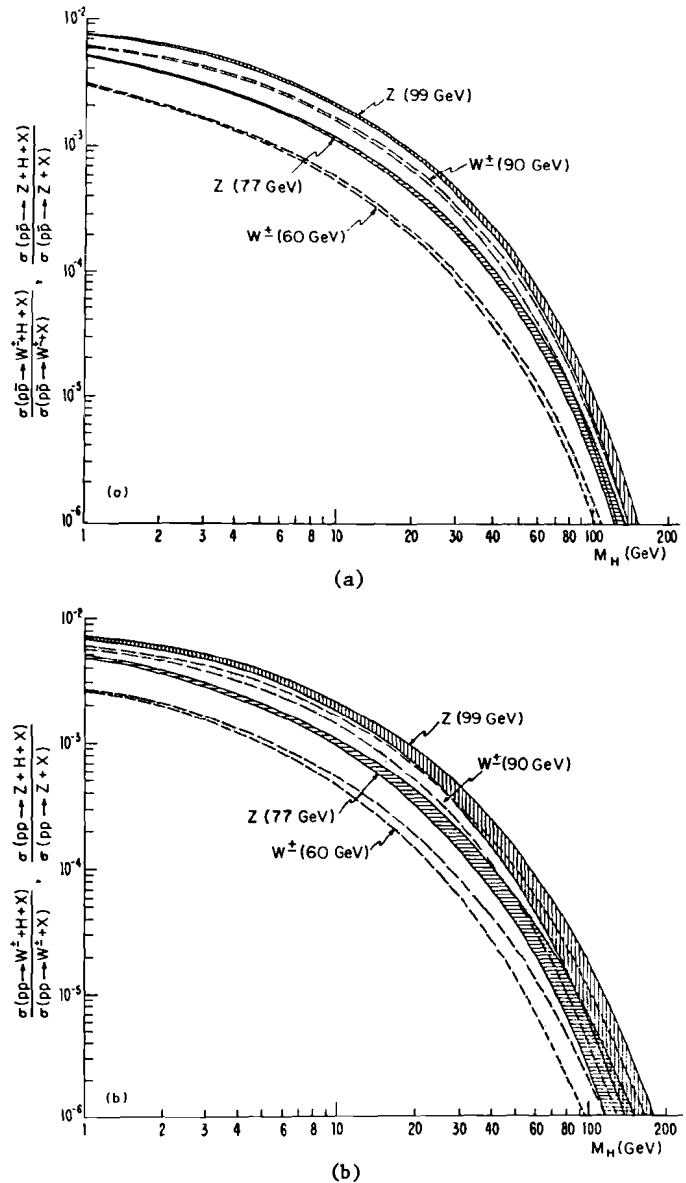


Fig. 5. Rate of associated production of the Higgs meson with W^\pm or with Z , versus m_H , expressed as a fraction of total W^\pm or Z production (from Ref. 21): (a) In $p\bar{p}$ collisions at $\sqrt{s} = 540$ GeV. (b) In pp collisions at $\sqrt{s} = 800$ GeV. Production with W^\pm is indicated by the dotted bands, with Z indicated by slashes. Bands are shown for $\mu_W = 60$ GeV ($\mu_Z = 77$ GeV) [lower curves] and for $\mu_W = 90$ GeV ($\mu_Z = 99$ GeV) [upper curves]. Bands indicate the range of variation due to different quark-distribution-function parametrizations.

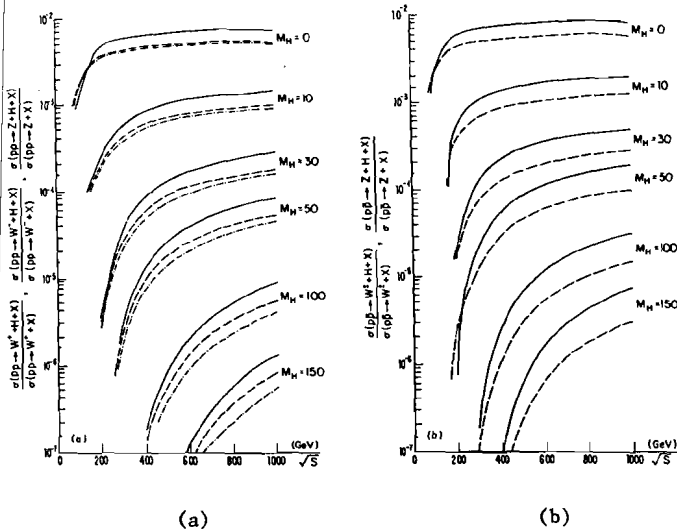


Fig. 6. Rate of associated production of the Higgs meson with W^+ , W^- , or Z , versus energy \sqrt{s} , expressed as a fraction of total W^+ , W^- , or Z production (from Ref. 21). (a) In $p\bar{p}$ collisions. (b) In pp collisions. Rates are shown for several M_H values, all using $\mu_w = 75$ GeV ($\mu_z = 86.6$ GeV).

III. Technicolor, Charged Higgses and All That

A. Motivations for Going Beyond the Standard Model

For as long as people have been investigating gauge models of the electroweak interactions, they have been unable to resist the temptation to generalize, complicate if you will, the standard model containing a single elementary Higgs doublet. Even within the strict confines of an $SU(2) \otimes U(1)$ gauge group and all the experiments supporting it, there is much room for generalization. In particular $SU(2) \otimes U(1)$ with any number of elementary Higgs doublets is consistent with all experiments.³

Two particularly good reasons for introducing more than one doublet have to do with CP-nonconservation. In the first, proposed by Lee²³ and Weinberg²⁴, the observed weak CP-violation is supposed to originate in the Higgs sector, either by spontaneous breakdown of CP-symmetry or by virtue of CP-nonconserving Higgs meson self-couplings. These mechanisms require two or three doublets at least. The second reason for introducing two or more doublets has to do with the problem of strong CP-violation induced by instantons.²⁵ Peccei and Quinn²⁶ showed that this problem can be eliminated by having at least two doublets related by a global $U(1)$ symmetry. As Weinberg and Wilczek²⁷ observed, this Peccei-Quinn symmetry implies the existence of an almost massless pseudoscalar, the axion, with couplings to ordinary matter comparable to those of H^0 (Eqs. (1) and (2)). This, apparently, introduces another problem, but we will not get into that here. Suffice it to say that no one has ever proposed a different, clearly workable solution to the strong CP-violation problem.

An $SU(2) \otimes U(1)$ model with two elementary Higgs doublets has eight spinless fields - four charged and four neutral. One neutral and two charged mesons are eaten by Z^0 and W^\pm in the Higgs mechanism, leaving behind as physical scalars H^\pm , H^0 , H^0' and H^0'' .²⁸ A model with three or more doublets has an even richer spectrum. The existence of one or more extra doublets implies additional freedom, in the form of mixing angles, in the couplings of H^\pm and the H^0 's to ordinary

matter so that, unfortunately, the precision of Eqs. (1) and (2) no longer holds. Rather than discuss them here, it is illuminating to compare and contrast these couplings with those of the technipions which will be introduced shortly. The discussion appears in Sec. III-C.

Finally, as in the case of the one-doublet model, the masses of Higgses in the multi-doublet models are almost completely unconstrained. On theoretical grounds, they must be ≤ 1 TeV.¹⁰ The fact that b -quark decays are not dominated by $b \rightarrow H^+c$ or H^+u implies that charged Higgses must be more massive than $m_b \approx 5$ GeV. That is all one can say.

In large part, it is this theoretical sloppiness with Higgs masses that has motivated the more ambitious attempts to go beyond the standard model - those associated with the terms dynamical symmetry breaking (technicolor/hypercolor) and supersymmetry (which we won't discuss here; see I. Hinchliffe's report in these proceedings).

Very briefly, "dynamical symmetry breaking" refers to the theoretical possibility of generating spontaneous breakdown of the electroweak gauge group $SU(2) \otimes U(1)$ to electromagnetic $U(1)$ ^{5,6} without the introduction of elementary Higgs multiplets. In this scenario, unlike elementary-Higgs models, the size of the Fermi constant, $G_F^{1/2} \approx 300$ GeV, has a simple dynamical origin: There is a new strong gauge interaction, technicolor, whose characteristic scale Λ_{TC} is analogous to Λ_{QCD} . Technifermions, analogous to quarks, interact via TC-boson exchange. Just like quarks, they acquire mass dynamically and, as a consequence of Goldstone's theorem, massless pseudoscalar bound states of technifermions are formed. If technifermions couple to $SU(2) \otimes U(1)$ in the same way that quarks and leptons do, i.e., one chirality in doublets, the other in singlets, then three of the massless "technipions" are eaten by W^\pm and Z^0 . The gauge bosons acquire mass $\mu_w = \frac{1}{2} g F_\pi$ and $\mu_z = \frac{1}{2} \sqrt{g^2 + g'^2} F_\pi \equiv \mu_w / \cos \theta_w$, where F_π is the technipion decay constant, analogous to $f_\pi = 95$ MeV for ordinary pions. Thus, $G_F/2 = g^2/8\mu_w^2 = 1/2F_\pi^2$ so that $F_\pi \approx 250$ GeV $\approx 2500 f_\pi$. In many respects, then, technicolor is just a scaled-up version of QCD; in particular, $\Lambda_{TC} \approx 2500 \Lambda_{QCD} = 0.5 - 1.0$ TeV.

At this point, there is a dramatic parting of the ways of elementary Higgs models and technicolor (TC) models. In the former there generally are just three massless Goldstone bosons, the unphysical ones eaten by W^\pm and Z^0 . The H^\pm and H^0 's left behind can, as noted, have almost any mass because free parameters in the Higgs self-interaction can be adjusted at will. In TC models, likewise, there are physical technipions left behind. Their mass is to a large extent precisely predicted because there are, in principle, no free parameters to adjust. Let us see how this comes about.

In all quasirealistic TC models constructed so far, there are at least four flavors of technihadrons of each chirality. This implies that there will be more than three massless Goldstone technipions formed when the technifermions acquire their dynamical mass. Only three are eaten; the rest remain as physical technipions which are strictly massless in the neglect of interactions which are weak compared to technicolor at scales of order Λ_{TC} .⁸ These weaker interactions do give mass to the physical technipions, that mass is calculable, and we believe we know what these interactions are. That is the basis of the statement that TC models have no free parameters.

The weaker interactions giving mass to technipions are the familiar color $SU(3)$ and the electroweak $SU(2) \otimes U(1)$ and a postulated new interaction known as

"extended technicolor" (ETC)⁷ or "sideways".⁸ The ETC interaction must be introduced to give ordinary quarks and leptons their observed nonzero current-algebra masses. This it accomplishes by introducing a gauge coupling which connects quarks and leptons to technifermions. The ETC gauge group is spontaneously broken at a scale of order 100 TeV (!) to a subgroup containing technicolor and ordinary color. (The value ~ 100 TeV is set by the TC scale, 1 TeV, and the magnitude of quark and lepton masses.) The contributions of these interactions to the mass of various technipions can be well-estimated using current-algebraic techniques.²⁹ The main uncertainty comes from the fact that no completely satisfactory TC model has yet been built, so that the ETC couplings are not precisely known. We shall summarize the mass estimates in the next subsection. For now, it is enough to say that the technipions corresponding most nearly to H^\pm and some of the H^0 's are predicted to have mass $\sim 5-40$ GeV, much less than the characteristic 1 TeV scale of technicolor.

We should also add here that ETC interactions are primarily responsible for the coupling of technipions to fermion-antifermion pairs. Thus, there is a certain amount of ignorance in calculating technipion decay branching ratios, just as there is for H^\pm and the H^0 's. Technipion couplings to electroweak gauge bosons are determined by the more well-known couplings of their constituent technifermions to W^\pm , Z^0 and γ . All this will be detailed soon.

Finally, there will be technicolor-neutral "technihadrons" analogous to the hadrons ρ , ω , ϵ and so on in QCD. The typical technihadron mass is ~ 1 TeV. Indeed, the precise analog of the neutral Higgs(es) which gives mass to quarks and leptons in elementary Higgs models is such a technihadron and, so, is unreachable in colliders of this decade.

B. The Technicolor Zoo-Particle Types, Charges and Masses

The number and quantum numbers of light technipions and heavy technihadrons is fixed, as in QCD, by the number of technifermion constituents and how they transform under technicolor. Obviously, this is a completely model-dependent issue, one which is far from being settled. In particular, technifermions may also carry ordinary color or not. Each technifermion belonging to an N -dimensional representation of color $SU(3)$ counts as N flavors since color $SU(3)$ is weak compared to technicolor.

To sample the richness possible in the TC-singlet spectrum, we shall consider a specific toy model proposed by Farhi and Susskind³⁰ and examined in some detail by Dimopoulos,³⁰ Peskin,³¹ and Preskill.³² The elementary technifermions in this model are a pair of techniquarks, $Q = (U, D)$, and a pair of technileptons, $L = (N, E)$. Both chirality components of U , D , N , E are assumed to transform according to the same unspecified, but nonreal, N_{TC} -dimensional representation of the technicolor gauge group, G_{TC} . Under $(SU(3), SU(2), U(1))$, they transform as follows:

$$Q_L = \begin{pmatrix} U \\ D \end{pmatrix}_L : (\underline{3}, \underline{2}, Y)$$

$$U_R : (\underline{3}, \underline{1}, Y + \frac{1}{2}); D_R : (\underline{3}, \underline{1}, Y - \frac{1}{2})$$

$$L_L = \begin{pmatrix} N \\ E \end{pmatrix}_L : (\underline{1}, \underline{2}, -3Y)$$

$$N_R : (\underline{1}, \underline{1}, -3Y + \frac{1}{2}); E_R : (\underline{1}, \underline{1}, -3Y - \frac{1}{2}). \quad (6)$$

The weak hypercharges assigned here guarantee that $G_{TC} \otimes SU(3) \otimes SU(2) \otimes U(1)$ gauge currents have no anomalous divergences. As usual, the electric charge is $Q_{EM} = T_{3,EW} + Y_{EW}$.

This specific model makes definite predictions of the number, charge and (approximate) mass of technipions and technihadrons. It is important that the reader understand that some, but not all, of these particles will exist in any other TC model.⁸ In particular, the lightest ones, called P^\pm , P^0 and P^0' below, occur in all models. Colored technipions will not exist in models in which all technifermions are ordinary color $SU(3)$ singlets. With this caveat, let us get on to cataloging the denizens of the zoo.

This version of the Farhi-Susskind model has an $SU(8) \otimes SU(8)$ chiral symmetry which is spontaneously broken down to $SU(8)$ by the dynamical technifermion masses. This implies $8^2 - 1 = 63$ Goldstone bosons, of which 3 are eaten by W^\pm and Z^0 . The remaining 60 physical technipions consist of 4 color singlets P^\pm , P^0 and P^0' , 24 color triplets P_{TQ} called leptoquarks, and 32 color octets P_8^\pm , P_8^0 and P_8^0' . The color-singlet technipions are most nearly analogous to the H^\pm and H^0 's. P_8^0' is often referred to as Π_T in the literature. The technifermion constituents, electric charge and mass of these spinless mesons are summarized in Table 1.³³ As far as their strong TC interactions and their coupling to gauge bosons are concerned, these particles are all pseudo-scalars. This is not generally true of their couplings to light fermionic matter, as we shall see.

TABLE 1. Technipions in the Farhi-Susskind model (Refs. 9,30,31,32). Q is the electric charge and T_3 the weak isospin of the technipion. Y is the weak hypercharge of the Q_L -doublet. For unit normalization, the states should be divided by $\sqrt{N_{TC}}$.

Technipion/Technifermion Content	Q	T_3	Estimated Mass (GeV)
<u>Color Singlets, P</u>			
$ P^+\rangle = \frac{1}{2\sqrt{3}} [U\bar{D}\rangle_{\underline{1}} - 3 N\bar{E}\rangle]$	1	1	7-40
$ P^-\rangle = P^+\rangle$	-1	-1	7-40
$ P^0\rangle = \frac{1}{2\sqrt{6}} [U\bar{U} - D\bar{D}\rangle_{\underline{1}} - 3 N\bar{N} - E\bar{E}\rangle]$	0	0	2-40
$ P^0'\rangle = \frac{1}{2\sqrt{6}} [U\bar{U} + D\bar{D}\rangle_{\underline{1}} - 3 N\bar{N} + E\bar{E}\rangle]$	0	0	2-40
<u>Color Triplet Leptoquarks, P_{TQ} ($\alpha = 1, 2, 3$)</u>			
$ P_{E\bar{U}}\rangle = E\bar{U}\rangle_{\underline{3}}$, $ P_{E\bar{D}}\rangle = E\bar{D}\rangle_{\underline{3}}$	$\pm(4Y+1)$	± 1	$\left. \begin{array}{l} \\ \\ \\ \end{array} \right\} 160\sqrt{\frac{4}{N_{TC}}}$
$ P_{N\bar{U}}\rangle = N\bar{U}\rangle_{\underline{3}}$, $ P_{N\bar{D}}\rangle = N\bar{D}\rangle_{\underline{3}}$	$\mp 4Y$	0	
$ P_{E\bar{D}}\rangle = E\bar{D}\rangle_{\underline{3}}$, $ P_{E\bar{U}}\rangle = E\bar{U}\rangle_{\underline{3}}$	$\mp 4Y$	0	
$ P_{N\bar{D}}\rangle = N\bar{D}\rangle_{\underline{3}}$, $ P_{N\bar{U}}\rangle = N\bar{U}\rangle_{\underline{3}}$	$\pm(4Y-1)$	± 1	
<u>Color Octets, P_{8a} ($a = 1, \dots, 8$)</u>			
$ P_8^+\rangle = U\bar{D}\rangle_{\underline{8}}$	1	1	$\left. \begin{array}{l} \\ \\ \\ \end{array} \right\} 240\sqrt{\frac{4}{N_{TC}}}$
$ P_8^-\rangle = P_8^+\rangle$	-1	-1	
$ P_8^0\rangle = \frac{1}{\sqrt{2}} U\bar{U} - D\bar{D}\rangle_{\underline{8}}$	0	0	
$ P_8^0'\rangle = \frac{1}{\sqrt{2}} U\bar{U} + D\bar{D}\rangle_{\underline{8}}$	0	0	

We have emphasized that these technipions are massless in the neglect of color SU(3), electroweak SU(2) \otimes U(1) and ETC interactions. The color-singlet P's acquire mass only from the latter two interactions and so they are the lightest technipions. The electroweak contribution can be calculated very reliably as it is completely model-independent.^{8,31,34,35} As with all such current-algebraic computations, one calculates the square of the mass. For P^\pm , the result is

$$\left(m_{P^\pm}^2\right)_{EW} = \frac{3\alpha}{4\pi} \mu_z^2 \ln \frac{\Lambda_{TC}^2}{\mu_z^2} = (7.0 - 8.5 \text{ GeV})^2 \quad (7)$$

for $\Lambda_{TC} = 0.5 - 1.0 \text{ TeV}$. For P^0 and P^0' ,

$$\left(m_{P^0, P^0'}^2\right)_{EW} \equiv 0. \quad (8)$$

While the ETC contribution to m_P^2 can, in principle, be fairly precisely calculated in a specific model, we believe we should give here a range of masses reflecting our ignorance of the "true model". If is^{8,35}

$$\left(m_{P^\pm}^2\right)_{ETC} \cong \left(m_{P^0}^2\right)_{ETC} \cong \left(m_{P^0'}^2\right)_{ETC} \cong (2 - 40 \text{ GeV})^2. \quad (9)$$

Using $m_P = \left[\left(m_{P^\pm}^2\right)_{EW} + \left(m_{P^\pm}^2\right)_{ETC} \right]^{\frac{1}{2}}$, the expected range of the lightest technipion masses is

$$m_{P^\pm} \cong m_{P^0} \cong m_{P^0'} \cong 10 - 40 \text{ GeV}$$

$$\text{if } \left(m_{P^\pm}^2\right)_{ETC} \gg \left(m_{P^\pm}^2\right)_{EW}, \quad (10)$$

or

$$m_{P^\pm} \cong 7 - 9 \text{ GeV},$$

$$m_{P^0} \cong m_{P^0'} \cong 2 - 3 \text{ GeV}$$

$$\text{if } \left(m_{P^\pm}^2\right)_{ETC} \ll \left(m_{P^\pm}^2\right)_{EW}. \quad (11)$$

The contribution of electroweak and ETC interactions to the masses of color triplet and octet technipions should be comparable to those just given. This is much less than the contributions from color SU(3), which have been estimated to be^{30,31,32}

$$m_{P_{LQ}} \cong 160 \sqrt{\frac{4}{N_{TC}}} \text{ GeV} \quad m_{P_8} \cong 240 \sqrt{\frac{4}{N_{TC}}} \text{ GeV}, \quad (12)$$

where N_{TC} is the dimensionality of the TC representation of the technifermions. Any model containing these technipions should give mass estimates not very different from these.

In Table 2, we have listed the $8^2 = 64$ ground-state technihadrons with spin one. They are all approximately degenerate at $\sim 900 \sqrt{\frac{4}{N_{TC}}} \text{ GeV}$. They are the most interesting technihadrons because some of them can be

produced in the very high energy colliders now being contemplated and because they provide a copious source of technipions.³⁶ The neutral color singlets ρ_2^0 and ω_1^0 have nonzero couplings to the photon and so appear as nearly degenerate s-channel resonances in e^+e^- annihilation. The color octet ω_8^0 mixes with color-SU(3) gluons and should be produced in $p\bar{p}$ and pp collisions at $\sqrt{s} \gtrsim 2 \text{ TeV}$. In each of their respective settings, these neutral mesons provide the principal way to access the heavy technipion pairs $P_8^+ P_8^-$ and $P_{LQ}^+ P_{LQ}^-$.

Before closing this discussion, we mention that a seemingly slight modification of the Farhi-Susskind model leads to a very different population of its technicolor zoo. Suppose, instead, that we had assigned the technifermions U, D, N, E to a real representation of the TC group whose symmetric product contains the TC-singlet representation.³⁷ Then there would be a total of 135 technipions - the 63 already mentioned and 72 more. The additional technipions consist of 6 color-singlet dileptons (LL) of mass 50 - 80 GeV, 24 color-triplet leptoquarks (LQ) and 6 color-triplet diquarks (QQ), all of mass $\sim 160 \text{ GeV}$, and 36 color-sextet diquarks of mass $\sim 400 \text{ GeV}$. Similar complications occur in the spin-one sector. The point, of course, is that the technipion spectrum can be very rich and that details are highly model-dependent.

TABLE 2. Lowest-lying spin-one technihadrons in the Farhi-Susskind model. All have mass $\cong 900 \sqrt{\frac{4}{N_{TC}}} \text{ GeV}$. W_L^\pm and Z_L^0 are longitudinal components of gauge bosons. For unit renormalization, states should be divided by $\sqrt{N_{TC}}$

Vector Technihadron/Technifermion Content	Q	Major Decay Modes
<u>Color Singlets</u>		
$ \rho_1^+\rangle = \frac{1}{\sqrt{3}} [U\bar{D}\rangle_{\frac{1}{2}} - 3 N\bar{E}\rangle]$	1	$\left\{ \begin{array}{l} P\bar{P}, P_{LQ}^+ P_{LQ}^-, \\ P_8^+ P_8^-, W_L^+ W_L^-, \\ W_L^\pm Z_L^0, \text{ etc.} \end{array} \right.$
$ \rho_1^-\rangle = \rho_1^+\rangle$	-1	
$ \rho_1^0\rangle = \frac{1}{\sqrt{6}} [U\bar{U} - D\bar{D}\rangle_{\frac{1}{2}} - 3 N\bar{N} - E\bar{E}\rangle]$	0	
$ \rho_2^+\rangle = \frac{1}{2} [U\bar{D}\rangle_{\frac{1}{2}} + N\bar{E}\rangle]$	1	
$ \rho_2^-\rangle = \rho_2^+\rangle$	-1	
$ \rho_2^0\rangle = \frac{1}{2\sqrt{2}} [U\bar{U} - D\bar{D}\rangle_{\frac{1}{2}} + N\bar{N} - E\bar{E}\rangle]$	0	
$ \omega_1^0\rangle = \frac{1}{2\sqrt{6}} [U\bar{U} + D\bar{D}\rangle_{\frac{1}{2}} - 3 N\bar{N} + E\bar{E}\rangle]$	0	3 Technipions and/or W_L^\pm, Z_L^0
$ \omega_2^0\rangle = \frac{1}{2\sqrt{2}} [U\bar{U} + D\bar{D}\rangle_{\frac{1}{2}} + N\bar{N} + E\bar{E}\rangle]$	0	
<u>Color Triplet Leptoquarks</u>		
$ \rho_{E\bar{U}}^+\rangle = \bar{E}U\rangle_{\frac{2}{3}}, \rho_{E\bar{U}}^-\rangle = \bar{E}U\rangle_{\frac{1}{3}}$	$\pm(4Y+1)$	$\left\{ \begin{array}{l} P_{LQ}^+ \bar{P}, P_{LQ}^- \bar{P}_8, \\ P_{LQ}^+ W_L^\pm, P_{LQ}^- Z_L^0 \end{array} \right.$
$ \rho_{N\bar{U}}^+\rangle = \bar{N}U\rangle_{\frac{2}{3}}, \rho_{N\bar{U}}^-\rangle = \bar{N}U\rangle_{\frac{1}{3}}$	$\pm 4Y$	
$ \rho_{E\bar{D}}^+\rangle = \bar{E}D\rangle_{\frac{2}{3}}, \rho_{E\bar{D}}^-\rangle = \bar{E}D\rangle_{\frac{1}{3}}$	$\pm 4Y$	
$ \rho_{N\bar{D}}^+\rangle = \bar{N}D\rangle_{\frac{2}{3}}, \rho_{N\bar{D}}^-\rangle = \bar{N}D\rangle_{\frac{1}{3}}$	$\pm(4Y-1)$	
<u>Color Octets</u>		
$ \rho_8^+\rangle = \bar{U}\bar{D}\rangle_{\frac{2}{3}}$	1	$\left\{ \begin{array}{l} P_8^+ \bar{P}_8, P_{LQ}^+ P_{LQ}^0 \end{array} \right.$
$ \rho_8^-\rangle = \bar{U}\bar{D}\rangle_{\frac{1}{3}}$	-1	
$ \omega_8^0\rangle = \frac{1}{\sqrt{2}} U\bar{U} - D\bar{D}\rangle_{\frac{2}{3}}$	0	
$ \omega_8^0\rangle = \frac{1}{\sqrt{2}} U\bar{U} + D\bar{D}\rangle_{\frac{2}{3}}$	0	

C. Couplings of Technipions and Higgses to Ordinary Matter

In most of the discussion that follows, we will not assume the scalar meson content of any particular elementary Higgs or technicolor model. In accord with our ignorance of the "correct" model, we shall allow for any number of neutral and singly-charged color-singlet scalar mesons. In the few instances that we specialize to the Farhi-Susskind model, that assumption will be made clear.

1. Elementary Higgses and Light Technipions

It is useful to discuss H^\pm and H^0 's together with P^\pm and P^0 's because their couplings to ordinary matter - quarks, leptons, electroweak bosons and gluons - are expected to be quite similar in some cases and completely different in others. The reason for this is that technipion couplings to light matter always occur through their constituent technifermions. Elementary Higgses, on the other hand, can have couplings to ordinary matter at the Lagrangian level, as in Eqs. (1) and (2), and some of these are expected to be much larger than the corresponding technipion couplings. If relatively light charged and neutral scalars are discovered, these differences should make it possible to determine whether they are elementary or composite.

Couplings to Fermions. The ETC interaction which connects technifermions to quarks and leptons is the mechanism by which technipions couple to light fermion-antifermion pairs. This is by far the largest coupling of any light color-singlet technipion to ordinary matter and, so, they will decay almost exclusively to such pairs. It is also true that elementary Higgses will decay exclusively to fermion and antifermion so long as $m_H \ll 2\mu_z$.

The effective interaction for the coupling of the i^{th} charged and neutral technipions, P_i^\pm and P_i^0 , to ordinary fermions has the general form (assuming no light right-handed neutrinos)³⁸

$$\begin{aligned} \mathcal{L}_{P_i f \bar{f}'} = & P_i^+ \sum_{r,s} \left\{ \bar{u}_r \left[A_{rsi}^\pm \left(\frac{1+\gamma_5}{2} \right) - B_{rsi}^\pm \left(\frac{1-\gamma_5}{2} \right) \right] d_s \right. \\ & \left. + \alpha_{rsi} \bar{\nu}_r \left(\frac{1+\gamma_5}{2} \right) \ell_s \right\} \\ & + P_i^0 \sum_{r,s} \left\{ \bar{u}_r \left[A_{rsi}^0 \left(\frac{1+\gamma_5}{2} \right) - B_{rsi}^0 \left(\frac{1-\gamma_5}{2} \right) \right] u_s \right. \\ & + \bar{d}_r \left[C_{rsi}^0 \left(\frac{1+\gamma_5}{2} \right) - D_{rsi}^0 \left(\frac{1-\gamma_5}{2} \right) \right] d_s \\ & \left. + \bar{\ell}_r \left[\beta_{rsi} \left(\frac{1+\gamma_5}{2} \right) - \gamma_{rsi} \left(\frac{1-\gamma_5}{2} \right) \right] \ell_s \right\} \\ & + \text{h.c.} \end{aligned} \quad (13)$$

The sums in Eq. (13) extend over all flavors r,s of quarks and leptons; there is also an implicit sum over quark colors. The dimensionless couplings $A_{rsi}^\pm, B_{rsi}^\pm, C_{rsi}^0, D_{rsi}^0, \beta_{rsi}, \gamma_{rsi}$, etc. are $\cong F_\pi^{-1}$ times a mass which is related in a complicated and model-dependent way to the current algebra mass of q_r, q_s or of ℓ_r, ℓ_s . Much of this complication is contained in unknown mixing-angle factors that arise from diagonalizing the mass matrices of quarks, leptons, technifermions and technipions. In general,

$A_{rsi}^\pm \neq B_{rsi}^\pm$ and so on.³⁹ Thus, even though technipions are pseudoscalars so far as their strong TC interactions are concerned, their light-fermion couplings are parity-violating. Moreover, it is generally not true that $F_\pi A_{rsi}^\pm \cong F_\pi B_{rsi}^\pm \cong m_{u_r} + m_{d_s}$ = sum of the current algebra masses of u_r and d_s .

Very similar remarks apply to the couplings of H^\pm and H^0 's to fermions. They depend on the number of Higgs doublets in the model and how these are chosen to couple to the fermion doublets and singlets. Models in which the Higgses are expected to be less massive than several hundred GeV generally are constructed according to the "natural flavor conservation" guidelines of Glashow and Weinberg.⁴⁰ In this class of models, all fermions having the same electric charge acquire their masses from the vacuum expectation value of only one of the Higgs doublets. (While a corresponding condition is not obviously necessary in TC theories, we shall effectively assume it for purposes of practical calculations of decay branching ratios.) Thus, in models with natural flavor conservation, the Higgs-fermion interaction looks like Eq. (13), but one can relate the coupling constants to fermion masses as follows:

$$\begin{aligned} F_\pi A_{rsi}^\pm &= (KM_d)_{rsi}^\pm A_{rsi}^\pm, \quad F_\pi B_{rsi}^\pm = (M_u K)_{rsi}^\pm B_{rsi}^\pm, \\ F_\pi \alpha_{rsi} &= m_{\ell_r} \alpha_i \delta_{rs} \end{aligned} \quad (14)$$

and

$$\begin{aligned} F_\pi A_{rsi}^0 &= \pm F_\pi B_{rsi}^0 = m_{u_r} A_i^0 \delta_{rs}, \\ F_\pi C_{rsi}^0 &= \pm F_\pi D_{rsi}^0 = m_{d_r} C_i^0 \delta_{rs}, \\ F_\pi \beta_{rsi} &= \pm F_\pi \gamma_{rsi} = m_{\ell_r} \delta_{rs} \beta_i. \end{aligned} \quad (15)$$

In Eqs. (14) and (15),

$$\begin{aligned} K &= \begin{pmatrix} K_{ud} & K_{us} & K_{ub} \\ K_{cd} & K_{cs} & K_{cb} \\ K_{td} & K_{ts} & K_{tb} \end{pmatrix} \\ &\cong \begin{pmatrix} 0.97 & -0.22 & -0.068 \\ 0.22 & 0.85 & 0.48 \\ 0.046 & 0.48 & 0.88 \end{pmatrix} \end{aligned} \quad (16)$$

is the usual Kobayashi-Maskawa^{41,42} matrix,

$$\begin{aligned} M_u &= \begin{pmatrix} m_u & & \\ & m_c & \\ & & m_t \end{pmatrix} = \begin{pmatrix} 5 \text{ MeV} & & \\ & 1.2 \text{ GeV} & \\ & & 20, 25 \text{ GeV (assumed)} \end{pmatrix} \\ M_d &= \begin{pmatrix} m_d & & \\ & m_s & \\ & & m_b \end{pmatrix} = \begin{pmatrix} 9 \text{ MeV} & & \\ & 175 \text{ MeV} & \\ & & 4.5 \text{ GeV} \end{pmatrix} \end{aligned} \quad (17)$$

are the diagonalized quark current algebra mass matrices³⁹ and m_{ℓ_r} is the mass of charged lepton ℓ_r . The

factors A_i, B_i, \dots, β_i are ratios of functions of Higgs-meson mixing angles. There are completely unknown. Because of these factors, the usual presumption that the Higgs coupling to $f+\bar{f}'$ goes like the mass of the heavier fermion of the pair is little more than a guess. The presumption is greater still for technipions. Nevertheless, it is a reasonable one, worth hanging on to until we are proven wrong.

To give some idea of the ranges one might expect for Higgs/technipion branching ratios, we have calculated them for four different "models" for the couplings A_{rsi}^\pm , etc. The first two models are based on the elementary Higgs couplings just discussed. We use Eqs. (13)-(15) with $A_i^0 = C_i^0 = \beta_i = 1$ and

$$A_i^\pm = B_i^\pm = \alpha_i = 1 \quad (\text{Model 1}) \quad (18a)$$

$$A_i^\pm = -B_i^\pm = \alpha_i = 1 \quad (\text{Model 2}) \quad (18b)$$

The second class of models is a (necessarily) crude attempt to represent simply the general calculations of technipion-fermion couplings in Ref. 38. We choose all P^0 couplings and those of P^\pm to $\ell^+\nu_\ell$ as in models 1 and 2; $P^\pm \rightarrow u_r \bar{d}_s$ amplitudes are taken to be

$$A_{rsi}^\pm = B_{rsi}^\pm = \sqrt{m_{u_r} m_{d_s}} / F_\pi \quad (\text{Model 3}) \quad (19b)$$

$$A_{rsi}^\pm = -B_{rsi}^\pm = \sqrt{m_{u_r} m_{d_s}} / F_\pi \quad (\text{Model 4}) \quad (19b)$$

For handy reference, the rate for $P_i^\pm \rightarrow u_r \bar{d}_s$ is

$$\Gamma(P_i^\pm \rightarrow u_r \bar{d}_s) = \frac{3p_{rs}}{16\pi} \left\{ |A_{rsi}^\pm + B_{rsi}^\pm|^2 \left(1 - \left(\frac{m_{ur} - m_{ds}}{m_p} \right)^2 \right) + |A_{rsi}^\pm - B_{rsi}^\pm|^2 \left(1 - \left(\frac{m_{ur} + m_{ds}}{m_p} \right)^2 \right) \right\}, \quad (20)$$

where p_{rs} is the quark momentum and the factor of 3 is due to the sum over quark colors. The factor of 3 is absent for decay to $\ell^+\nu_\ell$.⁴³

The branching ratios for a range of charged and neutral Higgs/technipion masses are listed in Tables 3 and 4. There we see the general tendency, built into the models, for P^\pm/H^\pm to decay into the heaviest possible quark-antiquark pair. Note, however, that in models 2 and 4 this tendency is sometimes foiled by phase space limitations. For $m_{p^\pm} \leq m_t$, the branching ratio for $P^\pm \rightarrow \tau^+\nu_\tau$ is fairly large, 10-20%; it generally drops to $\sim 1-4\%$ once decay to $t\bar{b}$ is allowed. We stress that

TABLE 3. Branching ratios for P^\pm/H^\pm decay to fermion + antifermion. The four values for each decay mode and mass refer to the four "models" for the couplings described in the text.

P^\pm/H^\pm Decay Mode ($m_t = 20$ GeV)	Branching Ratio (%) for				
	$m_\pm = 7.5$ GeV	10 GeV	20 GeV	30 GeV	40 GeV
$\tau^+\nu$	23.0, 26.5; 14.5, 23.5	18.5, 20.0; 11.0, 14.0	15.5, 16.0; 9.0, 9.5	1.0, 1.0; 1.5, 2.5	0.5, 0.5; 1.0, 1.0
$c\bar{s}$	24.5, 28.5; 6.0, 10.0	19.5, 21.0; 4.5, 5.5	16.0, 16.0; 3.5, 4.0	1.0, 1.0; 0.5, 1.0	0.5, 0.5; 0.5, 0.5
$c\bar{b}$	50.5, 43.0; 79.0, 66.0	61.0, 57.5; 84.0, 80.0	68.0, 67.0; 87.0, 86.5	3.5, 4.5; 13.0, 23.5	2.0, 2.0; 8.5, 10.5
$t\bar{s}$	—	—	—	21.0, 26.5; 3.0, 5.0	21.0, 23.0; 3.0, 4.0
$t\bar{b}$	—	—	—	73.5, 66.5; 82.0, 68.0	75.5, 73.0; 87.5, 83.5

P^\pm/H^\pm Decay Mode ($m_t = 25$ GeV)	Branching Ratio (%) for	
	$m_\pm = 30$ GeV	40 GeV
$\tau^+\nu$	2.5, 3.0; 3.5, 8.0	0.5, 0.5; 1.0, 1.5
$c\bar{s}$	2.5, 3.0; 1.5, 3.0	0.5, 0.5; 0.5, 0.5
$c\bar{b}$	10.5, 14.0; 36.5, 75.5	2.0, 2.0; 9.5, 14.0
$t\bar{s}$	29.5, 40.0; 3.0, 6.0	21.5, 24.0; 3.0, 4.5
$t\bar{b}$	54.0, 38.5; 55.5, 7.5	75.0, 72.0; 86.0, 79.5

TABLE 4. Branching ratios for P^0/H^0 decay to fermion + antifermion. The choice of signs in Eq.(15) makes no significant difference on the values obtained. Note that, for $m_0 > 2m_t$, $P^0/H^0 \rightarrow t\bar{t}$ is expected to be the dominant decay mode.

P^0/H^0 Decay Mode	Branching Ratio for $m_0 = 2.5 \text{ GeV}$	10 GeV	20 GeV	30 GeV	40 GeV
$\mu^+ \mu^-$	11	—	—	—	—
$\tau^+ \tau^-$	—	41	5	5	5
$s\bar{s}$	89	1	—	—	—
$c\bar{c}$	—	58	7	7	6
$b\bar{b}$	—	—	88	88	89

this $\tau^+ \nu_\tau$ mode, which is an important signal for charged scalars, is sizable because we have taken α_i comparable in magnitude to A_i^\pm and B_i^\pm . The real world may be quite different! Finally, the total width of a charged scalar is $\sim 0.01 - 0.1 \text{ MeV}$ for $m_\pm < m_t$ and $\sim 1 - 10 \text{ MeV}$ for $m_\pm > m_t$. Neutral scalar widths are comparable.

Couplings to Electroweak Gauge Bosons and QCD Gluons. Elementary Higgs mesons couple directly to Z^0 and W^\pm in the electroweak Lagrangian and so these interactions are fairly large. The most important terms for H^\pm and H^0 production are trilinear in the Higgs and electroweak fields. For any model containing two or more Higgs doublets, the nonvanishing elementary two-Higgs production amplitudes are:⁴⁴

$$\begin{aligned}
 A(\gamma(q) \rightarrow H_i^+(p) + H_j^-(k)) &= i e \delta_{ij} \epsilon(q) \cdot (p-k) \\
 A(Z^0(q) \rightarrow H_i^+(p) + H_j^-(k)) &= i e \delta_{ij} \cot 2\theta_w \epsilon(q) \cdot (p-k) \\
 A(Z^0(q) \rightarrow H_i^0(p) + H_j^0(k)) &= -i \frac{e}{\sin 2\theta_w} R_{ij}^{00} \epsilon(q) \cdot (p-k) \\
 A(W^+(q) \rightarrow H_i^0(p) + H_j^+(k)) &= i \frac{e}{2 \sin \theta_w} R_{ij}^{0+} \epsilon(q) \cdot (p-k) .
 \end{aligned} \tag{21}$$

Here, $\epsilon(q)$ is the gauge boson's polarization 4-vector, and R_{ij}^{00} and R_{ij}^{0+} are functions of the Higgs meson mixing angles. R_{ij}^{00} vanishes if $H_i^0 = H_j^0$. Note that, apart from the mixing angle factors, the coupling constants in Eq.(21) are just the electromagnetic, neutral weak and charged weak current charges Q , $T_3 - \sin^2 \theta_w Q$ and $g/2$ of the appropriate Higgs mesons.

The nonzero elementary amplitudes for bremsstrahlung of a Higgs meson from an electroweak boson are (cf. Eq.(2)):

$$\begin{aligned}
 A(Z^0(q) \rightarrow Z^0(p) + H_i^0(k)) &= \frac{2e\mu_z}{\sin 2\theta_w} \sum_j R_{ij}^0 \frac{v_j}{F_\pi} \epsilon(q) \cdot \epsilon(p) , \\
 A(W^\pm(q) \rightarrow W^\pm(p) + H_i^0(k)) &= \frac{e\mu_w}{\sin \theta_w} \sum_j R_{ij}^0 \frac{v_j}{F_\pi} \epsilon(q) \cdot \epsilon(p) ,
 \end{aligned} \tag{22}$$

where $v_i/\sqrt{2}$ is the vacuum expectation value of the i^{th} unmixed Higgs doublet φ_i appearing in the Lagrangian,

R_{ij}^0 is the matrix diagonalizing the neutral-Higgs mass matrix and $F_\pi = \sqrt{\sum_i v_i^2} \cong 250 \text{ GeV}$. Apart from this sum rule on the v_i , they are arbitrary. For making numerical estimates, we shall assume they are roughly equal in magnitude and not less than $\sim 100 \text{ GeV}$ (corresponding to ≤ 6 Higgs doublets). Note that there is no elementary coupling of γW^+ and $Z^0 W^+$ to physical charged Higgses. Thus, while $H^0 \rightarrow Z^0 Z^0$, $W^+ W^-$ dominates neutral Higgs decays when $m_{H^0} \geq 200 \text{ GeV}$, charged Higgses always decay predominantly to fermions. Also, as in the one-doublet case, the processes $Z^0 \rightarrow H^0 + \gamma$ and 2 gluons $- H^0$ must proceed through fermion loops and so are suppressed by \sim gauge coupling $\times m_f/F_\pi$ relative to Eqs.(22) unless there are very heavy fermions.

We turn now to the technipions. All of their interactions with electroweak and QCD gauge bosons proceed through technifermion loops. At energies well below their characteristic scale, Λ_{TC} , technipions are essentially point-like and these interactions are reliably calculated using well-known current-algebraic methods and the known technifermion-gauge boson couplings in, e.g., Eq.(6). (An example of the form factor effects that appear at production energies $\sim \Lambda_{TC}$ will be given in Secs. IV A,B.) Current algebra gives the γ , Z^0 , and W^\pm couplings to a pair of technipions as the charges eQ , $\sqrt{g^2 + g'^2} (\frac{1}{2} T_3 - \sin^2 \theta_w Q)$, and $g/2$, respectively, of their constituent technifermions. Thus,

$$\begin{aligned}
 A(\gamma - P_i^+ + P_j^-) &= i e \delta_{ij} \epsilon(q) \cdot (p-k) \\
 A(Z^0 - P_i^+ + P_j^-) &= i e \delta_{ij} \cot 2\theta_w \epsilon(q) \cdot (p-k) \\
 A(Z^0 - P_i^0 + P_j^0) &= 0 \\
 A(W^\pm - P_i^0 + P_j^\pm) &= i \frac{e}{2 \sin \theta_w} R'_{ij} \epsilon(q) \cdot (p-k)
 \end{aligned} \tag{23}$$

The first two amplitudes are the same as in Eqs.(21) because of the assumed electroweak quantum numbers of technifermions (Eq.(6)). Insofar as their assignment to $SU(2)_w$ doublets and singlets is required for a phenomenologically consistent TC theory, these amplitudes are model-independent. So is the third of Eqs.(23), which is our first important difference with elementary Higgs models. The fact that it vanishes in the current-algebra approximation means that it is suppressed by powers of $(m_{p0}/\Lambda_{TC})^2$ relative to other amplitudes in

Eq.(23). The quantity R'_{ij} in the last equation is a model-dependent mixing angle factor. In the simplest Farhi-Susskind model, $R'_{ij} = 1$ for P^0 and it vanishes for $P^{0'}$.

More striking departures from the elementary Higgs scenarios occur for the coupling of two gauge bosons to one technipion. The calculation of these are similar to that of the triangle anomaly graph for $\pi^0 \rightarrow \gamma\gamma$. The coupling of P to gauge bosons B_1 and B_2 is given by⁴⁵

$$\frac{\sqrt{2} S_{PB_1 B_2}}{8\pi^2 F_\pi} \epsilon_{\mu\nu\lambda\rho} \epsilon_1^\mu \epsilon_2^\nu P_1^\lambda P_2^\rho \quad (24)$$

where the triangle anomaly factor $S_{PB_1 B_2}$ is

$$S_{PB_1 B_2} = \frac{1}{2} g_1 g_2 \text{Tr}(Q_P \{Q_1, Q_2\}) \quad (25)$$

Here, $g_{1,2}$ are the $B_{1,2}$ gauge couplings and $Q_{1,2}$ their gauge charges. Q_P is the chiral charge of technipion P . The contributions from different gauge boson helicity states are summed separately in the trace. For the Farhi-Susskind model, we have listed the more important values of $S_{PB_1 B_2}$ in Table 5. For more complicated models, the anomaly factors are multiplied by different group-theoretic numbers and functions of technipion mixing angles. In any case, the values in Table 5 will not seriously mislead us.

From Table 5 and Eq.(22), we estimate

$$\left| \frac{A(Z^0 \rightarrow Z^0 P^0)}{A(Z^0 \rightarrow Z^0 H^0)} \right|^2 \cong 10^{-4} - 10^{-5} \quad (26)$$

Folding this into the rate for $e^+e^- \rightarrow Z^0_{\text{real}} \rightarrow H^0 \ell^+ \ell^-$ in Fig. 3, it is clear that the P^0 cannot be produced this way. To put it bluntly, observation of a narrow neutral scalar in this process rules out technicolor!

2. Heavy Technipions, $P_{L\bar{Q}}$ and P_8

Now that we have lavished so much time on light technipion couplings and, I hope, struck the correct note of uncertainty, we can deal with the heavy technipions in short order. We will discuss only the color-triplet leptoquarks $P_{L\bar{Q}}$ and octets P_8 of the simplest Farhi-Susskind model. We are even more unsure of their couplings to fermions (not to mention what fermion channels lie open to them, nor their very existence) than we are for their lighter cousins, and there seems little point in making more than conventional-wisdom guesses. This applies all the more strongly to the dileptons and diquarks found in the real-TC-representation version of the model, so we will not discuss them here. The interested (masochistic) reader can find them discussed in Refs. 30 and 11.

In view of their color SU(3) quantum numbers, we expect that the most important fermionic couplings of P_8 and $P_{L\bar{Q}}$ are of the form $A_{rs}^8 \sum_{a=1}^8 P_{8a} \bar{q}_r \lambda_a (1, \gamma_5) q_s$, where $\lambda_a = \text{color-SU(3) matrix}$, and

$A_{rs}^{L\bar{Q}} \sum_{a=1}^3 P_{L\bar{Q}^a} \alpha^a \bar{q}_r (1, \gamma_5) q_s \alpha^a$. Note that the latter coupling requires that $Y = 1/6$ in Eq.(6). The coefficients A_{rs}^8 are expected to be of order (heavier fermion mass $\times F_\pi^{-1}$). As one almost certainly too naive example,

TABLE 5. Anomaly factors $S_{PB_1 B_2}$ for the Farhi-Susskind model (from Ref. 45).

Vertex $PB_1 B_2$	Anomaly Factor $S_{PB_1 B_2}$
$P^0 \gamma\gamma$	$e^2 \frac{4}{\sqrt{6}} N_{TC}$
$Z^0 Z^0$	$-e^2 \frac{2 \cos^2 2\theta_w}{\cos^2 \theta_w} \frac{1}{\sqrt{6}} N_{TC}$
$Z^0 \gamma$	$e^2 \frac{2(1 - 4 \sin^2 \theta_w)}{\sin 2\theta_w} \frac{1}{\sqrt{6}} N_{TC}$
$W^+ W^-$	0
$P^{0'} G_a G_b$	$g_s^2 \frac{1}{\sqrt{6}} \delta_{ab} N_{TC}$
$\gamma\gamma$	$-e^2 \frac{4}{3\sqrt{6}} N_{TC}$
$Z^0 \gamma$	$e^2 \frac{4}{3\sqrt{6}} \tan \theta_w N_{TC}$
$Z^0 Z^0$	$-e^2 \frac{4}{3\sqrt{6}} \tan^2 \theta_w N_{TC}$
$W^+ W^-$	0
$P_{8a}^0 \gamma G_b$	$e g_s \delta_{ab} N_{TC}$
$Z^0 G_b$	$e g_s \cot 2\theta_w \delta_{ab} N_{TC}$
$P_{8a}^{0'} G_b G_c$	$g_s^2 \delta_{abc} N_{TC}$
γG_b	$e g_s \frac{1}{3} \delta_{ab} N_{TC}$
$Z^0 G_b$	$-e g_s \frac{1}{3} \tan \theta_w \delta_{ab} N_{TC}$

Barbiellini, et al.¹¹ take as the P_8 couplings appropriate to the Farhi-Susskind model:

$$i \frac{\sqrt{2}}{F_\pi} \sum_{\text{flavors}} \sum_{r,s} \left\{ P_{8a}^{0'} \left[m_u \bar{u}_r \gamma_5 \lambda_a u_r + m_d \bar{d}_r \gamma_5 \lambda_a d_r \right] \delta_{rs} \right. \\ \left. + P_{8a}^0 \left[m_u \bar{u}_r \gamma_5 \lambda_a u_r - m_d \bar{d}_r \gamma_5 \lambda_a d_r \right] \delta_{rs} \right. \\ \left. + P_{8a}^+ \bar{u}_r \left[(KM_d)_{rs} \left(\frac{1+\gamma_5}{2} \right) \lambda_a - (MK_u)_{rs} \left(\frac{1+\gamma_5}{2} \right) \lambda_a \right] d_s \right. \\ \left. + \text{h.c.} \right\} \quad (27)$$

On the basis of such expectations, it is commonly assumed that the largest color octet-to-fermion couplings

are $P_8^0 \rightarrow (t\bar{t})_8$, $P_8^+ \rightarrow (t\bar{b})_8$ and so on. Likewise, if $Y = 1/6$, $P_{\bar{E}U} \rightarrow \tau^+\tau$, $P_{\bar{N}U} \rightarrow \nu_\tau\tau$, etc. are presumed to be the largest leptoquark-fermion couplings. Since leptoquarks are color triplets these, in fact, are their dominant decay modes.

The couplings of a single gauge boson to a pair of heavy technipions are calculated using current algebra and gauge invariance, as before. We have listed the most interesting ones in Table 6 for the Farhi-Susskind model. However, the reader should note that these amplitudes generally are not directly useful for calculating production rates. At the center-of-mass energies required to pair-produce them, the amplitudes are expected to be dominated by spin-one technihadrons (see Sec. IV).

The color octet technipions can couple to a pair of gauge bosons. The amplitude is given in Eq.(24) and the anomaly factors $S_{P_8 B_1 B_2}$ included in Table 5.

The decay rate for $P_8 \rightarrow B_1 B_2$ is⁴⁵

$$\Gamma(P_8 \rightarrow B_1 B_2) = 2 \frac{\delta_{B_1 B_2} m_{P_8}^3}{128\pi} \left(\frac{\sqrt{2} S_{P_8 B_1 B_2}}{4\pi^2 F_\pi} \right)^2. \quad (28)$$

We can see from this that the P_8^0 -octet has an appreciable coupling to two gluons. Furthermore, using Eq.(27), we have

$$\frac{\Gamma(P_8^0 \rightarrow GG)}{\Gamma(P_8^0 \rightarrow (t\bar{t})_8)} = \frac{5}{3} \left(\frac{\alpha_s}{\pi} \right)^2 \left(\frac{m_{P_8}}{m_t} \right)^2 \left(\frac{N_{TC}}{4} \right)^2 \approx 0.25 \frac{N_{TC}}{4}, \quad (29)$$

where, again, N_{TC} is the dimensionality of the TC representation of techniquarks and we used $\alpha_s(m_{P_8}) \approx 0.1$ and $m_{P_8}/m_t \approx 12\sqrt{\frac{4}{N_{TC}}}$. Thus, P_8^0 (a.k.a. η_T) decays predominantly to $t\bar{t}$ and to two gluons. Since N_{TC} is unknown, we cannot be more specific than that.

This concludes our discussion of technipion and Higgs couplings to ordinary matter. In the next section we use these results to estimate the most likely means for their production and detection.

TABLE 6. Amplitudes of a single gauge boson coupled to a pair of heavy technipions in the Farhi-Susskind model. f_{abc} are the structure constants of SU(3) and λ^c are the matrices for the $\underline{3}$ representation, normalized to $\text{Tr} \lambda^c \lambda^d = 2\delta_{cd}$. The amplitude for $G_a + G_b \rightarrow P_{8c} + P_{8d}$ is $\frac{1}{2} g_s^2 (f_{ace} f_{bde} + f_{ade} f_{bce}) \epsilon_1 \cdot \epsilon_2$ times 2 for $P_8^+ P_8^-$ and times 1 for $P_8^0 P_8^0$ and $P_8^0 P_8^0$. The amplitude for $G_a + G_b \rightarrow P_{LQ\alpha} + P_{LQ\beta}$ is $\frac{1}{2} g_s^2 \{ \lambda^a, \lambda^b \}_{\alpha\beta} \epsilon_1 \cdot \epsilon_2$.

Technipion Pair	$\gamma [x e \epsilon(q) \cdot (p-k)]$	$Z^0 \times \frac{e}{\sin 2\theta_w} c \cdot (p-k)$	$G_c [x g_s \epsilon \cdot (p-k)]$
$P_8^+ P_8^-$	δ_{ab}	$\cos 2\theta_w \delta_{ab}$	f_{abc}
$P_{8a}^0 P_{8b}^0$	0	0	$\frac{1}{2} f_{abc}$
$P_{8a}^0 P_{8b}^0$	0	0	$\frac{1}{2} f_{abc}$
$P_{8a}^0 P_{8b}^0$	0	0	0
$P_{\bar{E}U\alpha} P_{\bar{E}U\beta}$	$(4Y+1)\delta_{\alpha\beta}$	$(1-2(4Y+1)\sin^2\theta_w)\delta_{\alpha\beta}$	$i \lambda_{\alpha\beta}^c / 2$
$P_{\bar{N}U\alpha} P_{\bar{N}U\beta}$	$4Y\delta_{\alpha\beta}$	$-8Y \sin^2\theta_w \delta_{\alpha\beta}$	$i \lambda_{\alpha\beta}^c / 2$
$P_{\bar{E}D\alpha} P_{\bar{E}D\beta}$	$4Y\delta_{\alpha\beta}$	$-8Y \sin^2\theta_w \delta_{\alpha\beta}$	$i \lambda_{\alpha\beta}^c / 2$
$P_{\bar{N}D\alpha} P_{\bar{N}D\beta}$	$(4Y-1)\delta_{\alpha\beta}$	$-(1+2(4Y-1)\sin^2\theta_w)\delta_{\alpha\beta}$	$i \lambda_{\alpha\beta}^c / 2$

IV. Production and Detection of Higgs Mesons and Technipions in Colliders

It is obvious that exploration of the scalar sector of electroweak interactions requires high-energy colliders. It is equally important that these colliders have consistently high luminosity. In this section we discuss in turn e^+e^- colliders, both at and below the Z^0 and colliding linacs at ultrahigh energies, the hadron-hadron colliders Isabelle and TEV I and ep colliders. We assume luminosities of 2×10^{31} for e^+e^- at the Z^0 and 10^{33} for colliding linacs, 10^{33} for pp at $\sqrt{s} = 800$ and 10^{30} for $\bar{p}p$ at $\sqrt{s} = 2000$, and 10^{32} for ep colliders at $\sqrt{s} = 300-1000$ GeV. Except in a few cases, we shall not dwell much on the all-important question of backgrounds; the reader is referred to the reports of the appropriate collider groups for details.

These are the principal conclusions of our study:

(1) Overall, e^+e^- colliders are the most effective and versatile. The existing and proposed machines can discover all scalars, elementary or composite, lighter than ~ 45 GeV. Taken together, studies at toponium and the Z^0 can decide between the elementary and technicolor scenarios. Ultrahigh energy colliding linacs copiously produce spin-one technihadrons as s-channel resonances and these decay exclusively to technipions, including the heavy colored ones.

(2) Hadron colliders such as Isabelle and TEV I produce at detectable levels only composite scalars, specifically those which couple strongly to gluons. They do the best (and soonest) job of singly-producing P_8^0/η_T and, possibly, P_8^0 . Colored technipion pairs may be produced at observable rates at TEV I, though not at Isabelle. Development of efficient high-resolution vertex detectors are essential for success in all these searches.

(3) ep colliders are limited to single-production of heavy colored technipions such as P_{LQ}^0 , P_8^0 and P_8^0 . However, observable rates probably require $\sqrt{s} \geq 1$ TeV.

(4) In almost all cases, accurate determination of scalar meson masses requires good jet identification, discrimination and mass resolution. The reason, of course, is that P^+ and H^+ are expected to decay mainly to $c\bar{b}$ or $t\bar{b}$, P^0 to $t\bar{t}$, etc. and these heavy quark jets will have to be distinguished from all others.

A. e^+e^- Colliders

The entire event structure is useful for detecting scalar mesons produced in e^+e^- annihilation. This fact makes e^+e^- the simplest and surest method for discovering them. In the following we discuss Higgs and technipion production in continuum e^+e^- annihilation, at toponium, at the Z^0 and at ultrahigh energies. We spell out how searches at toponium and the Z^0 can distinguish between the elementary and composite scenarios for the scalar sector and among various possibilities within each scenario.

Continuum Production. We noted in Sec. III that technipions are essentially point-like below $\sqrt{s} \approx \Lambda_{TC}$. Furthermore, the $\gamma, Z^0 \rightarrow P^+P^-$ and $\gamma, Z^0 \rightarrow H^+H^-$ amplitudes are identical and model-independent (Eqs.(21) and (23)). Thus, the charged-pair production cross section appropriate to this decade's generation of e^+e^- collider is

$$\frac{d\sigma(e^+e^- \rightarrow P^+P^- \text{ or } H^+H^-)}{d(\cos\theta)} = \frac{\pi\alpha^2}{8s} \beta^3 \sin^2\theta \left[|f_R(s)|^2 + |f_L(s)|^2 \right] \quad (30)$$

where $\beta = \sqrt{1-4m_{\pm}^2/s}$ is the meson velocity, θ the c.m. production angle and

$$f_R(s) = 1 - \frac{\cos 2\theta_w}{2 \cos^2 \theta_w} \frac{s}{s - \mu_z^2 + i\mu_z \Gamma_z} \quad (31)$$

$$f_L(s) = 1 + \cot^2 2\theta_w \frac{s}{s - \mu_z^2 + i\mu_z \Gamma_z}$$

We use $\mu_z = 93.0$ GeV and $\Gamma_z = 2.92$ GeV in calculations.⁴⁶ Two points that stand out in Eq.(31) are: (1) The continuum cross section is rather small; e.g., $R_{\pm}(s) = \sigma(e^+e^- \rightarrow P^+P^-)/\sigma(e^+e^- \rightarrow \mu^+\mu^-) \cong 0.14$ for $m_{\pm} = 10$ GeV and $\sqrt{s} = 35$ GeV. It should be remembered, however, that each distinct charged pair ultimately contributes 1/4 unit to R_{\pm} . (2) The angular distribution peaks at 90° . This fact is useful in searching for striking, though rare, signals and in event reconstruction.

The most striking signature of P^+P^-/H^+H^- production should be $P^+ \rightarrow$ hadrons ($c\bar{b}$, $c\bar{s}$, etc.) together with $P^- \rightarrow \tau^- \nu_\tau$. From Table 3, we would expect this class of decays to occur 20-40% of the time for $m_{\pm} < m_t$ and 1-10% of the time for $m_{\pm} > m_t$. In these events, at least $\sim 3/8$ of the total energy is missing in neutrinos. The degree of jettiness of the hadronic decay products of P^\pm depends both on β and the decay channels open to it. This fact requires sifting through different event samples for high- and low-mass searches. In 35% of these events, there will be a relatively low-energy, wide-angle isolated e or μ from τ -decay. Such events, though rare, are practically background-free. (This will be discussed in more detail when we take up the Z^0 .) In another 20% of these events, a single charged pion results from $\tau^- \rightarrow \pi^- \nu$ and $\rho^- \nu$. This, too, gives an isolated charged track if β is high enough.

Several groups at PETRA and PEP have already searched for charged scalars in both the $(\tau\nu)(q\bar{q})$ and $(\tau\nu)(\tau\nu)$ modes.⁴⁷ Upper limits on $B(P^\pm/H^\pm \rightarrow \tau^\pm \nu)$ ranging from 4 to 11% were obtained for 4 GeV $\leq m_{\pm} \leq 12$ GeV (see Fig. 7).⁴⁸ Only model 3 of Table 3 falls under these limits. Nevertheless, it is important to look for the $(q\bar{q})(q\bar{q})$ modes to completely rule out $m_{\pm} < 12$ GeV. It is worth remarking here that the all-hadrons mode most likely contains four charmed quarks, another striking signal if the technology exists to detect their decays.

Finally, continuum production of P^0 or H^0 is negligible. These neutral mesons are best searched for at toponium and the Z^0 , as we shall see.

Production at Toponium⁴⁹. Decays of the toponium ground state, $\zeta = 1^3S_1(\bar{t}t)$, may be a copious source of both charged and neutral scalars. If $m_t > m_{\pm} + m_b$, the semiweak transition $t \rightarrow P^+/H^+ + b$ is expected to be the dominant decay mode of the top quark. The decay rate is given by (for each charged meson)

$$\Gamma(t \rightarrow P^+ b) = \frac{p}{64\pi m_t^2} \left\{ |A_{tbi}^\pm + B_{tbi}^\pm|^2 \left((m_t - m_b)^2 - m_{\pm}^2 \right) + |A_{tbi}^\pm - B_{tbi}^\pm|^2 \left((m_t + m_b)^2 - m_{\pm}^2 \right) \right\} \quad (32)$$

For $m_t = 25$ GeV and $m_{\pm} = 15$ GeV, the four "models" of Sec. III (Eqs.(14)-(19)) give $\Gamma(t \rightarrow P^+ b)$ between 80 keV

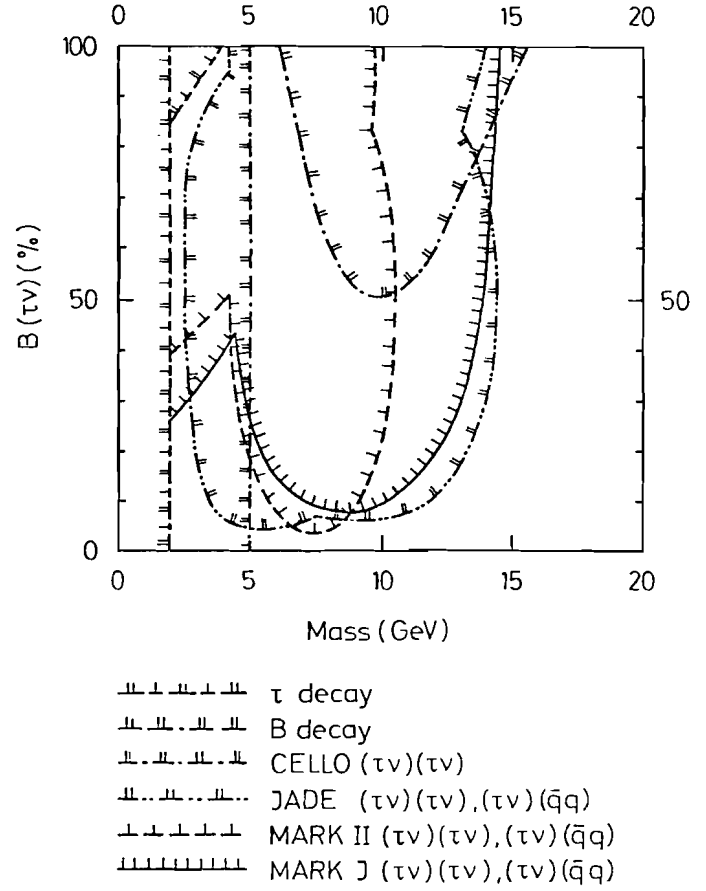


Fig. 7. Compilation of the limits on charged scalar branching ratios; from Ref. 47.

and 460 keV. The width of ζ expected in the standard quarkonium model is $\cong 60$ keV.⁵⁰ Thus, the first unmistakable signal that $m_t > m_{\pm} + m_b$ will be the extra large toponium width. Further, a large fraction of ζ decays will be

$$\zeta \rightarrow P^+ P^- b \bar{b} \rightarrow \begin{cases} 6 \text{ charmed quarks} \\ 4 \text{ charmed quarks} + \tau^\pm \\ 2 \text{ charmed quarks} + \tau^+ \tau^- \end{cases} \quad (33)$$

This would be impossible to miss with adequate vertex detectors.

Toponium is a good place to search for elementary H^0 's, in the decay $\zeta \rightarrow H^0 \gamma$. If the technicolor scenario is correct, it is the only place P^0 's can be found. (Remember that $m_{P^0} \leq 40$ GeV is almost certainly less than m_{ζ} .) The rate, relative to $\zeta \rightarrow e^+e^-$, is given by Eq.(4) times unknown mixing angle factors. Not all these factors can be much less than unity. Thus, if H^0 's or P^0 's exist and are less massive than ζ , they should be found in its radiative decays unless the branching ratio is much reduced by the existence of light charged scalars. We should always be faced with such alternatives!

Production at Z^0 . Two crucial tests for technicolor come at the Z^0 . First, if charged technipions exist, then $\mu_z > 2m_{P^\pm}$, and they should be pair-produced rather copiously there. For each distinct charged pair of scalars, Eqs.(21), (23), and (30) give

$$\begin{aligned} \sigma(e^+e^- \rightarrow Z^0 \rightarrow P^+P^- \text{ or } H^+H^-) \\ = \frac{\pi\alpha^2\beta^3}{6\Gamma_z^2} \frac{\cos^2 2\theta_w}{\sin^4 2\theta_w} (1 - 4\sin^2\theta_w + 8\sin^4\theta_w) \\ = 428 \beta^3 \text{ pb} \end{aligned} \quad (34a)$$

and

$$\begin{aligned} \Gamma(Z^0 \rightarrow P^+P^- \text{ or } H^+H^-) &= \frac{\alpha\mu_z\beta^3}{12} \cot^2 2\theta_w \\ &= 0.89 \times 10^{-2} \beta^3 \Gamma_z. \end{aligned} \quad (34b)$$

The angular distribution is proportional to $\sin^2\theta$.

As in the case of continuum production of charged scalars, the simplest signal to look for is e or μ + hadrons + missing energy. Unless the scalar is quite heavy, ~ 40 GeV, the hadrons should form one or two distinct jets and the lepton should be well isolated. Assuming 10^7 Z^0 's per year, Table 7 gives the expected annual yield of P^+P^- or H^+H^- and the number of these that end up in the signal mode. The $\tau^{\pm\nu}$ branching ratios used are an average of the appropriate ones in Table 3. The principal backgrounds to the e/μ + hadrons signal are discussed by Kagan.⁵¹ They are $Z^0 \rightarrow \tau^+\tau^-$, two-photon processes and $Z^0 \rightarrow t\bar{t}$. By requiring that the charged hadron multiplicity be ≥ 6 , that the missing momentum point into the detector, that e or μ not be within $\sim 60^\circ$ of another particle and other kinematic cuts, Kagan finds that these backgrounds are reduced below 0.03 pb, 0.1 pb and 0.1 pb, respectively. At most 30-50% of the signal is lost by these cuts. Furthermore, m_{\pm} can be determined to $\sim 10\%$ with existing detector technology.⁵² Thus, the Z^0 can be used to discover P^\pm or H^\pm up to 40 GeV in mass.

If $m_t > m_{\pm} + m_b$, another copious source of charged scalars will be

$$Z^0 \rightarrow t\bar{t} \rightarrow P^+P^- b\bar{b}. \quad (35)$$

Of course, this mode is much less clean than the simple $Z^0 \rightarrow P^+P^-$ decay. But, since it could yield $\sim 10^6$ P^+P^- events per year, detecting P^\pm in this way clearly warrants further careful study.

The second crucial test for technicolor involves the search for neutral scalar mesons in Z^0 decays. As we have stated before, neutral elementary Higgses arising from either single- or multi-doublet models can be found by missing-mass techniques in $e^+e^- \rightarrow Z^0 \rightarrow e^+e^-X$;

TABLE 7. Expected yield of P^+P^- or H^+H^- events at the Z^0 . P^+ or τ^+ branching ratios are taken from Table 3. The pairs of numbers for $m_{\pm} = 30$ GeV and 40 GeV correspond to $m_t = 20$ GeV (top) and $m_t = 25$ GeV (bottom).

m_{\pm} (GeV)	$\sigma(e^+e^- \rightarrow Z^0 \rightarrow P^+P^-)$ (pb)	Events per $10^7 Z^0$			$\sigma \cdot B$ (pb)
		P^+P^- Events	$\tau\nu$ + Hadrons	e^\pm or μ^\pm + Hadrons	
10	400	88×10^3	24×10^3	8.2×10^3	37.5
20	315	69×10^3	15×10^3	5.3×10^3	24.1
30	190	42×10^3	1.1×10^3	390	1.8
			3.4×10^3	1.2×10^3	5.4
40	57	12.5×10^3	175	60	0.3
			200	70	0.3

neutral technipions cannot (see Eq.(26)). Assuming no drastic suppression by mixing-angle factors, this search mode is sensitive to neutral Higgs masses up to ~ 45 GeV and, so, is the method of choice at the Z^0 .¹⁹

Another decay which leads to neutral Higgses, but not technipions, is $Z^0 \rightarrow H_i^0 H_j^0$ ($i \neq j$). From Eq.(21), the rate is

$$\Gamma(Z^0 \rightarrow H_i^0 H_j^0) = \frac{2\alpha |R_{ij}^{00}|^2}{3 \sin^2 2\theta_w} \frac{p^3}{\mu_z^2} = 0.23 |R_{ij}^{00}|^2 \left(\frac{p}{\mu_z}\right)^3 \Gamma_z. \quad (36)$$

A search for this decay would be more difficult than for $Z^0 \rightarrow P^+P^-/H^+H^-$. Naively, we expect the major H^0 decay modes to be $t\bar{t}$ (if allowed), $b\bar{b}$, $c\bar{c}$ and $\tau^+\tau^-$.⁵³ Probably the best signal is $H_i^0 \rightarrow q\bar{q}$ together with $H_j^0 \rightarrow \tau^+\tau^-$, leading to e^\pm or μ^\pm + hadrons + missing energy ($E_{\text{miss}} > 3/16 \mu_z$). I am not aware of any careful study of the best signals and attendant backgrounds for this two-Higgs decay of Z^0 ; one should be carried out.

To sum up, scalar meson searches at the Z^0 can distinguish between the various elementary and composite scenarios for the Higgs sector. If neutral scalars are found in either of the two decay modes just discussed, then technicolor is definitely ruled out. The same is true if charged scalar pairs are not found in Z^0 decays. Observation of $Z^0 \rightarrow H_i^0 H_j^0$ tells us that there are 2 or more elementary Higgs doublets. Finally, observation of charged, but not neutral, scalars at the Z^0 very strongly suggests that the technicolor scenario is correct. We could take it as proved, moreover, if a neutral scalar also is seen in radiative toponium decays.

Production at Ultrahigh Energies. We assume for this discussion the eventual existence of an e^+e^- colliding linac capable of covering the energy range $\sqrt{s} = 0.5 - 1.5$ TeV with an average luminosity of 10^{33} $\text{cm}^{-2} \text{sec}^{-1}$ for 10^7 sec per year. One unit of R at 1 TeV amounts to 865 events per year.⁵⁴ It is likely that only the technicolor scenario can provide a spectacularly obvious and simple signal of scalar mesons in such a machine, namely the production of technihadrons as s-channel resonances and their subsequent decay to technipion pairs. Moreover, this is the only significant mechanism for producing heavy colored technipions in e^+e^- annihilation. For definiteness, we restrict our discussion to the mesons listed in Tables 1 and 2 for the Farhi-Susskind model. Other models should give at least qualitatively similar results.

At energies of order Λ_{TC} , technipions can no longer be considered point-like, and form factors enter their production amplitudes. In ultrahigh energy e^+e^- annihilation, these form factor effects should be adequately described by vector-technimeson dominance. The lowest lying technihadrons coupling to e^+e^- through the γ and Z^0 are ρ_2^0 and ω_1^0 of Table 2. Note that they are very nearly degenerate at $m_{\rho_T} \cong 900 \sqrt{\frac{4}{N_{TC}}} \text{ GeV}$. Each of these decay to a pair of charged technipions and a pair of longitudinal W 's, $W_L^+ W_L^-$. The pair-production cross section has been calculated by Peskin.⁵⁵ Relative to the point cross section, $4\pi\alpha^2/3s$, he obtained

$$\begin{aligned} R_{TC}(s) &= \sum_i R_{\text{asy}}(e^+e^- \rightarrow P_i^+ \bar{P}_i^-) \beta_i^3 m_{\rho_T}^4 \\ &\times \left[\left(s - m_{\rho_T}^2 \right)^2 + \left(\frac{g_p^2}{96\pi} N_F s \sum_j f_j \beta_j^3 \right)^2 \right]^{-1}, \end{aligned} \quad (37)$$

where

$$R_{\text{asy}}(e^+e^- \rightarrow P_i \bar{P}_i) = \frac{1}{8} \left[Q + \frac{\cos 2\theta_w}{\sin^2 2\theta_w} (T_3 - 2Q \sin^2 \theta_w) \right]^2 + \frac{1}{8} \left[Q - \frac{2 \sin^2 \theta_w}{\sin^2 2\theta_w} (T_3 - 2Q \sin^2 \theta_w) \right]^2 \quad (38)$$

is the asymptotic contribution of $P_i \bar{P}_i$ to R_{TC} . Q and T_3 are the electric charge and weak isospin of P_i (see Table 1), $\beta_i = (1 - 4m_{P_i}^2/s)^{1/2}$, f_i is the fraction of $\lim_{s \rightarrow \infty} R_{\text{TC}}(s)$ associated with P_i and $g_p^2 N_F / 96\pi = 0.75$ for $N_F = 8$ technifermion flavors. Notice that Peskin has used an s -dependent width in Eq.(37).

The energy dependence of R_{TC} is shown in Fig. 8 for $N_{\text{TC}} = 4$ and $Y = 1/6$. While the technihadron mass nominally is at 900 GeV, we see that the resonance appears at ~ 800 GeV with a width of ~ 350 GeV. More important, $R_{\text{TC}} \cong 22$ at the resonance peak, an enhancement of 5 over what it would be at 800 GeV without the ρ_{T} . This corresponds to 30,400 technipion pairs per year. The relative fractions of technipions at the peak are

$$P^+P^- : W_L^+W_L^- : \sum_{\bar{L}Q} P_{\bar{L}Q} P_{L\bar{Q}} : P_8^+P_8^- \\ = \beta_P^3 : \beta_W^3 : 10.4 \beta_{P_{\bar{L}Q}}^3 : 8.0 \beta_{P_8}^3 \\ \cong 1.00 : 0.95 : 8.10 : 4.15 \quad (39)$$

Note that we are summing over the four species of leptosquarks in Eq.(39).

These events will be spectacular. All angular distributions are proportional to $\sin^2 \theta$. The P^+P^- events should appear as two narrow approximately back-to-back jets of unusually low invariant mass or as a narrow jet with $\tau^\pm \nu$ on the other side. $W_L^+W_L^-$ usually will give two rather broader jets or one jet plus $\ell^\pm \nu$.

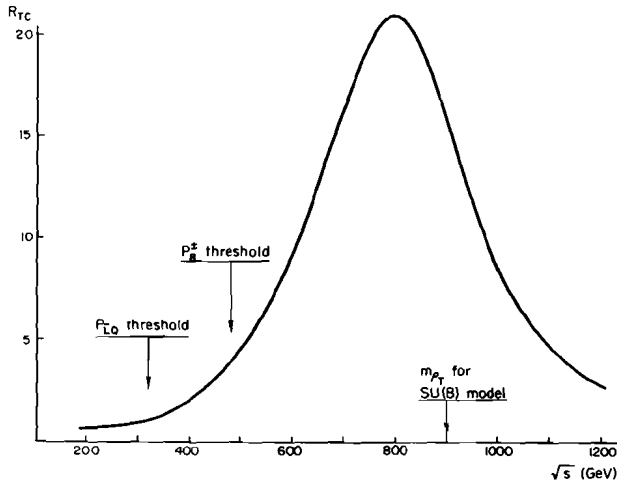


Fig. 8 The technipion contribution to R in the TeV-region of e^+e^- annihilation, assuming the Farhi-Susskind model. Taken from Ref. 55.

The principal background to these events, $e^+e^- \rightarrow W^+W^-$, contributes about 20 units to R . However, it is dominated by t -channel ν_e -exchange, so it is strongly peaked the forward direction and should be relatively easy to subtract.⁵⁴ The leptosquarks each will give a quark (t ?) jet plus a charged lepton (τ ?) or neutrino on the same side. Here, the missing energy will be considerable, 25-50% of \sqrt{s} . These events will never give back-to-back jets and will be easy to distinguish from P^+P^- and $W_L^+W_L^-$. The color octet P_8^+ is expected to decay to $t\bar{b}$. Thus, in the $P_8^+P_8^-$ events there should appear on each side a narrow b -jet plus a broader jet or two jets from the t -quark. The opening angle between the b - and t -jets will be $\leq 25^\circ$. Again, these events will be clearly distinguishable from the others and from backgrounds.

In closing, we remind the reader that the results presented here were for one specific model - one which we know cannot be correct in detail. Thus, our discussion should be viewed as only exemplary of what to expect if technicolor is correct. If it is, the details may be quite different, but there must be spin-one resonances in the TeV region of e^+e^- annihilation and these will decay to technipion and $W_L^+W_L^-$ pairs.

B. Hadron-Hadron Colliders

Exploration of the scalar sector by pp and $\bar{p}p$ colliders is limited to those mesons which couple relatively strongly to gluons. As we have stated and will re-emphasize here, this means that these colliders cannot see any elementary Higgs mesons and they will have to depend on the essential correctness of the technicolor scenario to make a positive discovery here. The most promising cases for Isabelle and TEV I are two-gluon fusion of P_8^0 ' and possibly, P_0 '. Furthermore, production of heavy colored technipion pairs may be observable at TEV I, though probably not at Isabelle. Let us discuss single- and pair-production of technipions in turn.

P_8^0 ' Production. In principal, of course, hadron colliders can produce the elementary H^0 and the technipions P_0 ' and P_8^0 ', and it is instructive to compare the three. The differential cross section for production of a scalar meson S^0 of mass m_0 by gluon fusion is^{20,35}

$$\frac{d\sigma}{dy}(pp \text{ or } \bar{p}p \rightarrow S^0 + X) = \frac{\pi^2}{8} \frac{\Gamma(S^0 \rightarrow GG)}{m_0^3} G(x_1)G(x_2) \quad (40)$$

where $G(x)$ is the gluon distribution function, x_1 and x_2 are the fractions of longitudinal momentum carried by the gluons and y is the rapidity of S^0 :

$$y = \frac{1}{2} \ln \left(\frac{E_0 + P_{0L}}{E_0 - P_{0L}} \right) = \frac{1}{2} \ln \frac{x_1}{x_2}; \\ x_1 = \frac{m_0}{\sqrt{s}} e^y, \quad x_2 = \frac{m_0}{\sqrt{s}} e^{-y} \quad (41)$$

Ignoring mixing-angle factors that would arise in any but the simplest models, the two-gluon widths are (see Ref. 20, Eq.(18) and Table 5):

$$\frac{\Gamma(S^0 \rightarrow GG)}{m_0^3} = \frac{\alpha_s^2(m_0)}{2\pi^3 F_\pi^2} \times \begin{cases} \frac{1}{4} \left(\frac{N_f}{3} \right)^2 & \text{for each } H^0 \\ \frac{4}{3} \left(\frac{N_{\text{TC}}}{4} \right)^2 & \text{for each } P_0' \\ \frac{5}{3} \left(\frac{N_{\text{TC}}}{4} \right)^2 & \text{for each } P_8^0' \end{cases} \quad (42)$$

For purposes of comparison, we take $m_{H^0} = m_{P_0'} = 20$ GeV

and $\alpha_s(20 \text{ GeV}) = 0.25$; $m_{P_8^0} = 240 \text{ GeV}$ and $\alpha_s(240 \text{ GeV}) = 0.1$; and $N_f = 3$, $N_{TC} = 4$. Using the popular choice $G(x) = 3(1-x)^5$, we get

$$\left. \frac{d\sigma(H^0)}{dy} \right|_{y=0} = \frac{9\alpha_s^2}{64\pi F_\pi^2} \left(1 - \frac{m_{H^0}}{\sqrt{s}}\right)^{10} \cong \begin{cases} 14 \text{ pb at } \sqrt{s} = 800 \text{ GeV} \\ 16 \text{ pb at } \sqrt{s} = 2000 \text{ GeV} \end{cases} \quad (43)$$

$$\left. \frac{d\sigma(P_8^0)}{dy} \right|_{y=0} = \frac{3\alpha_s^2}{4\pi F_\pi^2} \left(1 - \frac{m_{P_8^0}}{\sqrt{s}}\right)^{10} \cong \begin{cases} 74 \text{ pb at } \sqrt{s} = 800 \text{ GeV} \\ 86 \text{ pb at } \sqrt{s} = 2000 \text{ GeV} \end{cases} \quad (44)$$

$$\left. \frac{d\sigma(\sum_a P_8^0)}{dy} \right|_{y=0} = \frac{15\alpha_s^2}{2\pi F_\pi^2} \left(1 - \frac{m_{P_8^0}}{\sqrt{s}}\right)^{10} = \begin{cases} 4.3 \text{ pb at } \sqrt{s} = 800 \text{ GeV} \\ 42 \text{ pb at } \sqrt{s} = 2000 \text{ GeV} \end{cases} \quad (45)$$

In Sec. II we were pessimistic about detecting H^0 in its $c\bar{c}$, $b\bar{b}$ and $\tau^+\tau^-$ decay modes for cross sections as small as those in Eq. (43). For the same mass, the P_8^0 cross section is 16/3 times larger and this may be enough to warrant a serious study of detecting it in these modes. We urge that this be done (and apologize in advance if we are ignorant of someone's already having done it). The cross sections for P_8^0 production are also fairly small. Here, however, the expectation that P_8^0 decays predominantly to $t\bar{t}$ ($B_{t\bar{t}} > 50\%$) is cause for optimism, as we discuss next.

Figure 9 shows the total P_8^0 cross section at $\sqrt{s} = 800 \text{ GeV}$ and 2000 GeV .⁵⁶ They differ by a factor of ~ 30 -60 in the interesting mass range $m_{P_8^0} = 200$ -300 GeV. However, the assumed Isabelle and TEV I luminosities,

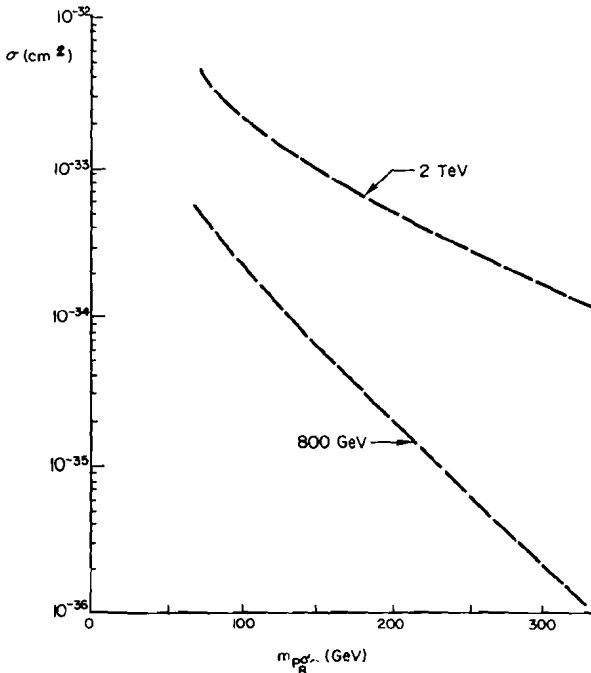


Fig. 9. The total P_8^0 production cross section expected at Isabelle ($\sqrt{s} = 800 \text{ GeV}$) and TEV I ($\sqrt{s} = 2000 \text{ GeV}$); from Ref. 56.

10^{33} and $10^{30} \text{ cm}^{-2} \text{ sec}^{-1}$ respectively, turn the tables. For $m_{P_8^0} = 240 \text{ GeV}$, one expects $\sim 75,000 P_8^0$ produced per year at Isabelle, only ~ 3000 at TEV I.

These events are to be searched for in the $t\bar{t}$ decay mode. The nonleptonic decays of t and \bar{t} , comprising $\sim 45\%$ of all $t\bar{t}$ events, generally give two narrow jets each with little missing energy. Assuming a finely segmented hadronic calorimeter (say, $5^\circ \times 5^\circ$ cells) and large angles between the t - and \bar{t} -jets, Baltay estimated a 4-jet invariant mass resolution of $\Delta m/m \cong 3\%$ at $m \cong 200 \text{ GeV}$. This estimate may be optimistic now, but one may hope that it will become realistic as experience is gained in single- and multi-jet mass reconstruction.

The main backgrounds to $P_8^0 \rightarrow t\bar{t}$ - jets are light quark and gluon jets with high transverse momentum (p_\perp) and heavy quark ($c\bar{c}$, $b\bar{b}$ and $t\bar{t}$) jets. The background levels expected for a 10^7 second run at Isabelle are shown in Fig. 10 along with estimates of the signal for $m_{P_8^0} = 200 \text{ GeV}$ and 300 GeV . To obtain a useful signal/background level requires: (1) triggering on 4 or more jets (2 or 3 on each side) in which each pair of jets has high invariant mass, of order m_t ; and (2) development of efficient high-resolution vertex detectors to tag the charm decays from $t \rightarrow b \rightarrow c$. Since only $\sim 5\%$ of high- p_\perp light quark and gluon jets contain a $c\bar{c}$ pair, requiring charm on both sides reduces this background by a factor of $2.5 e_c^2 \times 10^{-3}$, where e_c is the charm

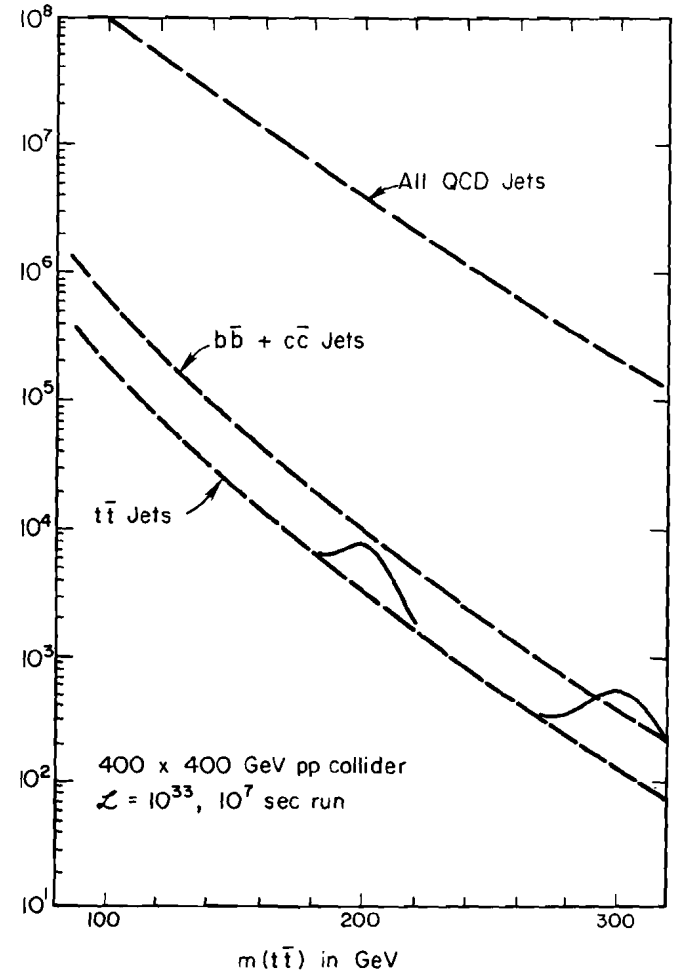


Fig. 10. Background levels to $P_8^0 \rightarrow t\bar{t}$ - jets at Isabelle, with $\int \mathcal{L} dt = 10^{40} \text{ cm}^{-2}$. The bumps are the expected P_8^0 signal for $m_{P_8^0} = 200$ and 300 GeV . Taken from Ref. 56.

detection efficiency of the vertex device. It is expected that requiring that the shape or effective mass of jet pairs be consistent with a t -quark origin will further reduce this background and the $c\bar{c}$, $b\bar{b}$ jet backgrounds by $\sim 1/3$. A glance at Fig. 10 shows that these rejection factors are sufficient.

Figure 11 shows the results of a hypothetical search for a 300 GeV P_8^0 at Isabelle. To obtain this,² Baltay assumed $B(P_8^0 \rightarrow t\bar{t})B(t\bar{t} \rightarrow 4 \text{ jets}) = (0.85)(0.6)^2$, $\epsilon_c = 0.85$ and various geometric cuts, all of which led to an estimated 10% detection efficiency for $P_8^0 \rightarrow t\bar{t}$.⁵⁷ Folding in this estimate with the P_8^0 production cross sections (Fig. 9) and the assumed Isabelle and TEV I luminosities results in Table 8 comparing the event rates at the two machines. It is clear from this table that P_8^0 , if it exists, can be found at Isabelle so long as the vertex detector efficiency does not fall below $\sim 10\%$; success at TEV I will require $\sim 50\%$ efficiency.

$P_8^0 P_8^0$ and $P_{LQ} P_{LQ}$ Production. Color SU(3) gauge invariance implies the one- and two-gluon couplings to $P_8^0 P_8^0$ and $P_{LQ} P_{LQ}$ given in Table 6. Thus, these pairs can be produced in high energy hadron-hadron collisions. The basic subprocesses are $GG \rightarrow P\bar{P}$ and $q\bar{q} \rightarrow P\bar{P}$; the latter is important only for $p\bar{p}$ collisions when $\sqrt{s} \cong 1$ -2 TeV. The naive lowest-order graphs are shown in Fig. 12.⁵⁸ At high enough energies, the indicated s -channel graphs in Fig. 12 should be vector-meson dominated by the coupling of G_a to the technihadron ω_{8a}^0 . Eichten has calculated the pair production cross sections including this effect as well as that of estimated scaling violations.⁵⁹ Unfortunately, Isabelle and TEV I

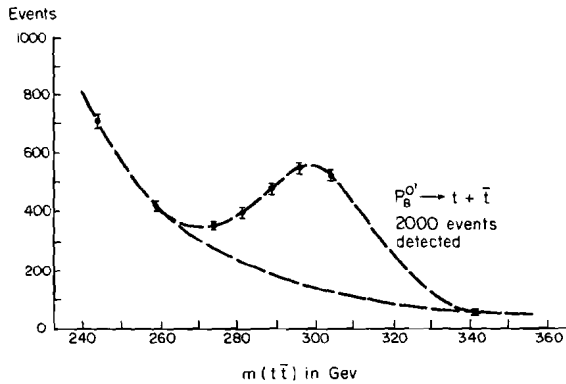


Fig. 11. Results of a hypothetical search for P_8^0 at Isabelle with $\sqrt{s} = 800$ GeV, $\int \mathcal{L} dt = 10^{40} \text{ cm}^{-2}$; from Ref. 56.

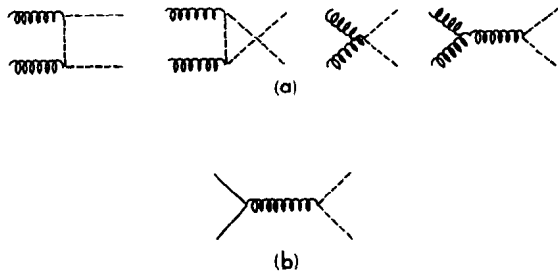


Fig. 12. Feynman graphs for the subprocesses (a) $GG \rightarrow P\bar{P}$ and (b) $q\bar{q} \rightarrow P\bar{P}$. Curly lines are gluons, dashed lines are technipions and solid lines are quarks. The fourth graph in (a) and graph (b) are dominated by the ω_{8a}^0 pole at high energies.

TABLE 8. P_8^0 production and detection rate comparison for Isabelle ($\sqrt{s} = 800$) and TEV I ($\sqrt{s} = 2000$). (Ref. 56.)

m_{P_8} (GeV)	$\sqrt{s} = 800 \text{ GeV}, \int \mathcal{L} dt = 10^{40}$			$\sqrt{s} = 2000 \text{ GeV}, \int \mathcal{L} dt = 10^{37}$		
	σ (pb)	Total Events	Detected Events	σ (pb)	Total Events	Detected Events
100	200	2×10^6	2×10^5	2000	2×10^4	2×10^3
200	20	2×10^5	2×10^4	500	5×10^3	500
300	2	2×10^4	2×10^3	150	1.5×10^3	150
400	0.2	2×10^3	200	60	600	60

energies are still too low for the ω_{8a}^0 to have a dramatic effect on the subprocesses. Eichten finds that the $p\bar{p} \rightarrow P\bar{P}X$ cross section is increased by $\sim 50\%$ and the $pp \rightarrow P\bar{P}X$ cross section by only 10%. His results for the $P_8^0 P_8^0$ and $P_{LQ} P_{LQ}$ cross sections, per channel, are shown in Fig. 13 for Isabelle and Fig. 14 for TEV I.

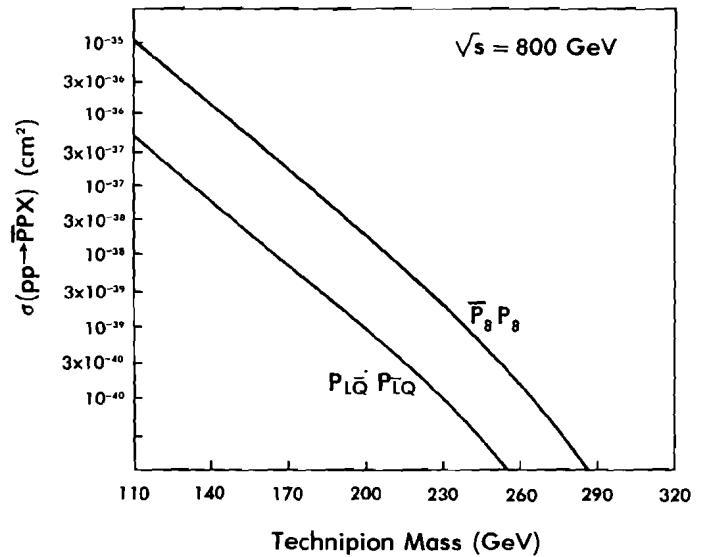


Fig. 13. The cross section for $P_{LQ} P_{LQ}$ and $P_8^0 P_8^0$ production at Isabelle ($\sqrt{s} = 800$ GeV) as a function of technipion mass; from Ref. 59.

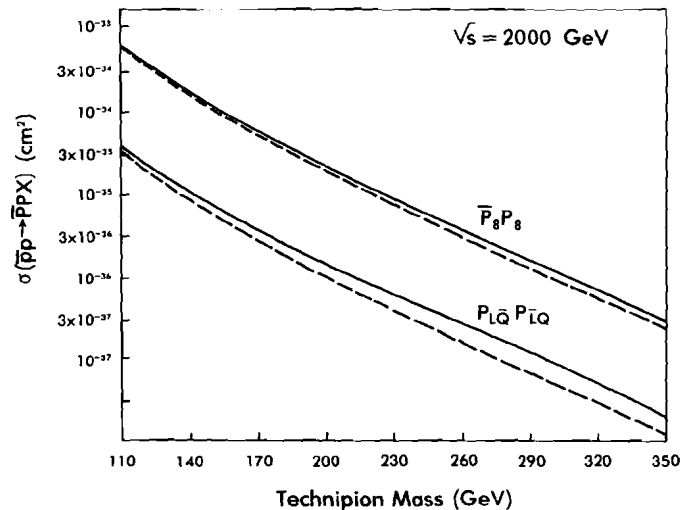


Fig. 14. The cross section for $P_{LQ} P_{LQ}$ and $P_8^0 P_8^0$ production at TEV I ($\sqrt{s} = 2000$ GeV) as a function of technipion mass. The dashed curves do not include ω_{8a}^0 ; from Ref. 59.

For the technipion mass range of interest, the cross sections expected at Isabelle are:

$$\sigma(pp \rightarrow P_{LQ}^- P_{LQ}^+ X) \cong \begin{cases} 2.9 \times 10^{-38} \text{ cm}^2 & (m_{P_{LQ}} = 150 \text{ GeV}) \\ 0.5 \times 10^{-38} \text{ cm}^2 & (m_{P_{LQ}} = 175 \text{ GeV}) \end{cases} \quad (46a)$$

$$\begin{aligned} \sigma(pp \rightarrow P_8^+ P_8^- X) &= \sigma(pp \rightarrow (P_8^0 P_8^0 + P_8^0 P_8^0) X) \\ &\cong \begin{cases} 2.9 \times 10^{-39} \text{ cm}^2 & (m_{P_8} = 225 \text{ GeV}) \\ 0.4 \times 10^{-39} \text{ cm}^2 & (m_{P_8} = 250 \text{ GeV}) \end{cases} \end{aligned} \quad (46b)$$

The expected cross sections at TEV I are:

$$\sigma(\bar{p}p \rightarrow P_{LQ}^- P_{LQ}^+ X) \cong \begin{cases} 7.1 \times 10^{-36} \text{ cm}^2 & (m_{P_{LQ}} = 150 \text{ GeV}) \\ 3.1 \times 10^{-36} \text{ cm}^2 & (m_{P_{LQ}} = 175 \text{ GeV}) \end{cases} \quad (47a)$$

$$\begin{aligned} \sigma(\bar{p}p \rightarrow P_8^+ P_8^- X) &= \sigma(\bar{p}p \rightarrow (P_8^0 P_8^0 + P_8^0 P_8^0) X) \\ &\cong \begin{cases} 1.0 \times 10^{-35} \text{ cm}^2 & (m_{P_8} = 225 \text{ GeV}) \\ 0.5 \times 10^{-35} \text{ cm}^2 & (m_{P_8} = 250 \text{ GeV}) \end{cases} \end{aligned} \quad (47b)$$

Thus, for this particular technicolor model, one can expect at most a few hundred leptoquark pairs of each species and practically no color octet pairs produced per year at Isabelle. The decay topologies are similar to those discussed for heavy technipion pair production in ultrahigh energy e^+e^- annihilation. Clearly, this meager sample of events will be swamped by backgrounds. The number of technipion pairs of each type will be no more than 50-100 at TEV I. There the background levels will be 1000 times smaller than at Isabelle so that, with adequate calorimetry and vertex detection, they may be observable.

In our discussion of e^+e^- annihilation at ultrahigh energies, we closed with a remark cautioning the reader not to rely too heavily on the detailed results of any specific technicolor model. The same applies here, of course. Even if technicolor is correct, there is no guarantee that technifermions carry ordinary color - a necessary condition for the existence of heavy colored technipions. If they do carry color, they may belong to representations other than the triplet. This possibility would lead to a richer spectrum of technipions, with different masses and production cross sections than used here. Finally, it is important to keep in mind that there is an inherent uncertainty in calculations of technipion production in hadron colliders. The correct parametrizations of the gluon distribution function and of scaling violations and the choice of Λ_{QCD} are far from settled issues. Different choices can and do lead to appreciably different cross section estimates.

C. ep Colliders

If color triplet leptoquarks exist, they can be found in ep collisions, if the colliders have high enough energy and luminosity and adequate detectors. It may also be possible to photoproduce color octet technipions. Here we assume $\mathcal{L}_{ep} = 10^{32} \text{ cm}^{-2} \text{ sec}^{-1}$ for

10^7 seconds per year.

The naive expectations that leptoquarks couple to fermions like ordinary charged Higgses leads one to the conclusion that their production in ep collisions is dominated by the subprocess shown in Fig. 15. The cross section has been calculated by Rudaz and Vermaseren.⁶⁰ They take the $\bar{e}tP_{E\bar{U}}$ coupling constant to be $\sqrt{2} G_{\frac{1}{2}}^2 m_t R_{et}$, where R_{et} is an unknown mixing angle factor. Assuming $m_{P_{LQ}} = 160 \text{ GeV}$ and $m_t \cong 20 \text{ GeV}$, they find

$$\sigma(ep \rightarrow P_{E\bar{U}} + t + X) \cong \begin{cases} 3 |R_{et}|^2 \text{ pb at } \sqrt{s} = 310 \text{ GeV} \\ 13 |R_{et}|^2 \text{ pb at } \sqrt{s} = 800 \text{ GeV} \end{cases} \quad (48)$$

The naive expectation also suggests $|R_{et}|^2 \ll 1$. If this is correct, then prospects for leptoquark production at HERA ($\sqrt{s} = 310 \text{ GeV}$) are slim. Clearly, a high-energy machine, $\sqrt{s} \cong 1 \text{ TeV}$, is required for this job. Such high ep energies are, in fact, achievable by a "cheap" modification of the e^+e^- colliding linacs discussed earlier.⁵⁵

Photoproduction of P_8^0 and P_8^0 in ep colliders has been proposed by Grifols and Mèndez.⁶¹ The basic subprocesses they considered were $\gamma + G \rightarrow P_8^0$ and P_8^0 , where the photon is quasireal. The γP_8 couplings were given in Table 5. For a gluon distribution function $G(x) = 3(1-x)^5$, they obtained

$$\begin{aligned} \sigma\left(\gamma p \rightarrow \begin{Bmatrix} P_8^0 \\ P_8^0 \end{Bmatrix} + X\right) &= \begin{Bmatrix} 1 \\ 1/9 \end{Bmatrix} \times 6 \left(1 - \frac{m_{P_8}^2}{s}\right)^5 \frac{\alpha_s \alpha_s(m_{P_8})}{2\pi F_{\pi}^2} \left(\frac{N_{TC}}{4}\right)^2 \\ &\cong \begin{Bmatrix} 4.5 \\ 0.5 \end{Bmatrix} \left(1 - \frac{m_{P_8}^2}{s}\right)^5 \left(\frac{N_{TC}}{4}\right)^2 \text{ pb} \end{aligned} \quad (49)$$

where our canonical estimate $\alpha_s(m_{P_8}) \cong 0.1$ was used. The subprocesses $Z^0 + G \rightarrow P_8^0$ and P_8^0 were overlooked by Grifols and Mèndez, but they will not increase the production rates by more than a factor of 2 at very high energies. If we assume an effective γp luminosity of $10^{31} \text{ cm}^{-2} \text{ sec}^{-1}$, we see that one can expect only $\sim 10 P_8^0$ produced per year at HERA energies.

We conclude that probes of the scalar sector by ep colliders require center-of-mass energies of the order of 1 TeV.

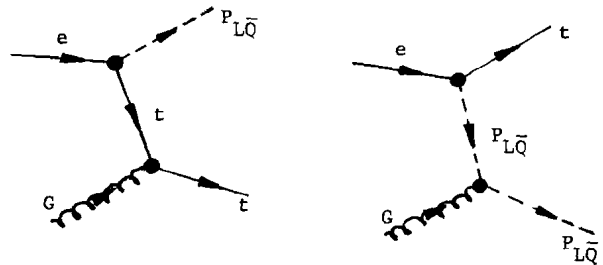


Fig. 15. Dominant mechanism for technileptoquark production in ep collisions (taken from Ref. 60).

Acknowledgements

In one way or another, this report could not have been written without the help, encouragement and information supplied me by the following people: Charlie Baltay, Joanne Day and her marvelous colleagues, Bob Diebold, Estia Eichten, Bernie Gittelman, Kurt Gottfried, Ian Hinchliffe, Harris Kagan, Gordy Kane, Jacques Leveille, Steve Olsen, Frank Paige, Dave Pellett, Marty Perl, Michael Peskin, Abe Seiden, Maury Tigner, and Helmut Wiedemann. In other words, I am indebted to the A.P.S. Division of Particles and Fields for its wonderfully stimulating Summer Study. I am also grateful to the Theory Group at CERN for its hospitality and facilities during the initial stages of writing the report. Finally, preparing the report would have been impossible without the amazing typing skill of Phyllis Dolan and the patience and cuisine of Kathy Cox.

This work was supported in part by the Department of Energy under Contract No. AC02-76ER01545.

References and Footnotes

1. S.L. Glashow, Nucl. Phys. 22, 579 (1961); S. Weinberg, Phys. Rev. Lett. 19, 1264 (1967); A. Salam, in Proceedings of the 8th Nobel Symposium on Elementary Particle Theory, Relativistic Groups and Analyticity, edited by N. Svartholm (Almqvist and Wiksells, Stockholm, 1968), p.367.
2. J. Schwinger, Phys. Rev. 125, 397 (1962); 128, 2425 (1962); P.W. Anderson, Phys. Rev. 130, 439 (1963); P. Higgs, Phys. Rev. Lett. 12, 132 (1964); 13, 508 (1964); F. Englert and R. Brout, Phys. Rev. Lett. 13, 321 (1964); G.S. Guralnik, C.R. Hagen and T.W.B. Kibble, Phys. Rev. Lett. 13, 585 (1964).
3. From measurement of neutral-current and charged-current deep-inelastic neutrino-nucleon cross sections, it is inferred that $\rho \equiv \mu_w^2/\mu_z^2 \cos^2 \theta_w = 1.00 \pm 0.03$ (see, e.g., J.E. Kim, et al., Rev. Mod. Phys. 53, 211 (1981)). The only natural way to have $\rho = 1$ in the standard model is spontaneous gauge symmetry breaking induced by elementary or composite Higgs doublets alone.
4. The urgency of this problem has been emphasized by L.B. Okun, in Proceedings of the 1981 International Symposium on Lepton and Photon Interactions at High Energies, edited by W. Pfeil (Bonn, 1981).
5. S. Weinberg, Phys. Rev. D13, 974 (1976); D19, 1277 (1979).
6. L. Susskind, Phys. Rev. D20, 2619 (1979).
7. S. Dimopoulos and L. Susskind, Nucl. Phys. B155, 237 (1979).
8. E. Eichten and K. Lane, Phys. Lett. 90B, 125 (1980).
9. E. Farhi and L. Susskind, Phys. Rev. D20, 3404 (1979).
10. J. Ellis, M.K. Gaillard and D.V. Nanopoulos, Nucl. Phys. B106, 292 (1976); G. Barbiellini, et al., "The Production and Detection of Higgs Particles at LEP", DESY Report 79/27 (1979).
11. K.D. Lane and M.E. Peskin, in Proceedings of the XV^{me} Rencontre de Moriond (J. Tran Thanh Van, ed.), Vol. II, 469 (1980); P. Sikivie, "An Introduction to Technicolor", Lectures given at the International School of Physics "Enrico Fermi", Varenna (1980); E. Farhi and L. Susskind, Phys. Rep. 74C, 277 (1981); K. Lane, "Hyperpions at the Z⁰", in Proceedings of the Cornell Z⁰ Theory Workshop, edited by M.E. Peskin and S.-H.H. Tye, p.435 (1981); G. Barbiellini, et al., "Technicolor Particles at LEP", DESY Report 81-064 (1981).
12. It is customary to assign weak hypercharge 1/2 to φ so that the doublet may be written $\varphi = \begin{pmatrix} \varphi_1^+ \\ \varphi_0^+ \end{pmatrix}$. Assuming the vacuum expectation value $\langle \varphi \rangle = \begin{pmatrix} 0 \\ v/\sqrt{2} \end{pmatrix}$, where $v = v^* = 2^{-\frac{1}{2}} G_F^{-\frac{1}{2}}$, implies that the observable neutral Higgs is $H^0 = (\varphi^0 + \varphi^{0\dagger})/\sqrt{2} - v$.
13. For a discussion of and references to the bounds on m_H , see G. Barbiellini, et al., Ref. 10.
14. V. Barger, F. Halzen and W.Y. Keung, U. Wisconsin-Madison Preprint MAD/PH/27.
15. J. Ellis, M.K. Gaillard, D.V. Nanopoulos and C.T. Sachrajda, CERN Preprint TH-2634 (1979).
16. F. Wilczek, Phys. Rev. Lett. 39, 1304 (1977).
17. J.D. Bjorken, in Proceedings of the 1976 SLAC Summer Institute, edited by M.C. Zipf (1976).
18. R. Cahn, M. Chanowitz and N. Fleishon, Lawrence Berkeley Laboratory Preprint LBL-8495 (1978).
19. M. Goldberg, in Report of the 100 GeV Facility Subgroup of the e⁺e⁻ Collider Group, these proceedings.
20. H.M. Georgi, S.L. Glashow, M.E. Machacek and D.V. Nanopoulos, Phys. Rev. Lett. 40, 692 (1978).
21. S.L. Glashow, D.V. Nanopoulos and A. Yildiz, Phys. Rev. D18, 1724 (1978).
22. L.-L. Chau Wang, "Highlights of High Energy pp, p \bar{p} and e⁺e⁻ Interactions", in Proceedings of the Cornell Z⁰ Theory Workshop, edited by M.E. Peskin and S.-H. H. Tye, p.302 (1981).
23. T.D. Lee, Phys. Rev. D8, 1226 (1973).
24. S. Weinberg, Phys. Rev. Lett. 37, 657 (1976).
25. G. 't Hooft, Phys. Rev. Lett. 37, 8 (1976); R. Jackiw and C. Rebbi, Phys. Rev. Lett. 37, 172 (1976); C. Callan, R. Dashen and D. Gross, Phys. Lett. 63B, 334 (1976).
26. R.D. Peccei and H.R. Quinn, Phys. Rev. Lett. 38, 1440 (1977); Phys. Rev. D16, 1791 (1977).
27. S. Weinberg, Phys. Rev. Lett. 40, 223 (1978); F. Wilczek, Phys. Rev. Lett. 40, 279 (1978).
28. In models with two Higgs doublets, φ_1 and φ_2 , the unphysical combinations are $i[v_1(\varphi_1^0 - \varphi_1^{0\dagger}) + v_2(\varphi_2^0 - \varphi_2^{0\dagger})]/\sqrt{2(v_1^2 + v_2^2)}$ and $(v_1\varphi_1^\pm + v_2\varphi_2^\pm)/\sqrt{v_1^2 + v_2^2}$, where $\langle \varphi_1 \rangle = \begin{pmatrix} 0 \\ v_1/\sqrt{2} \end{pmatrix}$ and $\sqrt{v_1^2 + v_2^2} = 2^{-\frac{1}{2}} G_F^{-\frac{1}{2}}$. The physical Higgs mesons are $H^\pm = (v_2\varphi_1^\pm - v_1\varphi_2^\pm)/\sqrt{v_1^2 + v_2^2}$, $H^{0''} = i[v_2(\varphi_1^0 - \varphi_1^{0\dagger}) - v_1(\varphi_2^0 - \varphi_2^{0\dagger})]/\sqrt{2(v_1^2 + v_2^2)}$, while H^0 and $H^{0'}$ are (model-dependent) orthogonal linear combinations of $(\varphi_1^0 + \varphi_1^{0\dagger})/\sqrt{2} - v_1$ and $(\varphi_2^0 + \varphi_2^{0\dagger})/\sqrt{2} - v_2$.
29. For a review of these techniques, see S. Weinberg, "The Problem of Mass" in a "A Festschrift for I.I. Rabi" (New York Academy of Sciences, 1977) p.185.
30. S. Dimopoulos, Nucl. Phys. B168, 69 (1980).

31. M.E. Peskin, Nucl. Phys. B175, 197 (1980).
32. J.P. Preskill, Nucl. Phys. B177, 21 (1981).
33. To avoid the possibility of absolutely stable color-triplet leptoquarks, it is generally assumed that $Y = 1/6$. While we are not sure there is a problem if $Y = 1/6$ (e.g., if $Y = 1/12$, a bound state of $\overline{P}_{\overline{U}}^{\pm}$ and \overline{u} is a color singlet fermion with charge $2/3!$), we shall use that value in practical calculations.
34. J.D. Bjorken, unpublished calculations.
35. S. Dimopoulos, S. Raby and G.L. Kane, Nucl. Phys. B182, 77 (1981).
36. As indicated in Table 2, color singlet technihadrons decay with full strength into W_L^{\pm} and Z_L^0 , the longitudinal components of the electroweak gauge bosons. The reason for this is that these components really are just the three unphysical technipions absorbed in the Higgs mechanism (see Ref. 6).
37. This, in fact, is what happens in the original version of the Farhi-Susskind model, Ref. 9.
38. K.D. Lane, unpublished calculations.
39. To have $A_{rsi}^{\pm} = B_{rsi}^{\pm}$, ETC interactions would have to be parity conserving, in which case charge $2/3$ and $-1/3$ quarks would be degenerate in pairs (Ref. 8). This is not unique to ETC models; the couplings of elementary charged Higgs mesons to fermions must be parity-violating for the same reason.
40. S.L. Glashow and S. Weinberg, Phys. Rev. D15, 1958 (1977).
41. M. Kobayashi and K. Maskawa, Prog. Theor. Phys. 49, 652 (1973).
42. I thank S. Rudaz for the compilation of KM angles used in Eq.(16). For recent discussions of bounds on the angles, see R. Shrock, S. Treiman and L.-L. Wang, Phys. Rev. Lett. 42, 1589 (1979); S. Pakvasa, S.F. Tuan and J.J. Sakurai, Phys. Rev. D23, 2799 (1981).
43. Two remarks are in order here: (i) It is possible that the enhancement of $q\overline{q}$ modes brought about by the color factor of 3 in Eq.(20) is ameliorated by Clebschs in the $A_{rsi}^{\pm,0}$, $B_{rsi}^{\pm,0}$, etc. For example, in one model considered in G. Barbiellini, et al. (Ref. 11), couplings to quarks are reduced by a factor of 3 relative to those to leptons. In another model, however, they are increased by a relative factor of 3. We have taken a moderate middle road in our models, but it is easy to modify the numbers in Tables 3 and 4 to reflect such factors. (ii) We have assumed flavor-conserving couplings of neutral technipions to quark and lepton pairs. We remind the thorough reader that it is just possible that this is not the case and that some neutral technipions may prefer such decay modes as $t\overline{c}$ or $c\overline{t}$, $b\overline{s}$ or $s\overline{b}$, etc.
44. In terms of the original unmixed fields φ_i (see Ref. 28), the interaction giving the third of Eqs.(21) is $\frac{ie}{\sin 2\theta_w} Z^\mu \varphi_i^0 \overleftrightarrow{\partial}_\mu \varphi_i^{0\dagger} = \frac{2e}{\sin 2\theta_w} Z^\mu \text{Re } \varphi_i^0 \overleftrightarrow{\partial}_\mu \text{Im } \varphi_i^0$ (summed over i). The mass eigenstates H_j^0 generally are linear combinations of some or all of the $\text{Re } \varphi_i^0$ and $\text{Im } \varphi_i^0$. In Eq.(22), only the real parts $(\varphi_i^0 + \varphi_i^{0\dagger})/\sqrt{2} - v_i$ contribute to the interaction term.
45. J. Ellis, M.K. Gaillard, D.V. Nanopoulos and P. Sikivie, Nucl. Phys. B182, 529 (1981).
46. W. Marciano and Z. Parsa, "Z⁰ Decay", in Proceedings of the Cornell Z⁰ Theory Workshop, edited by M.E. Peskin and S.-H.H. Tye, p.127 (1981).
47. J. Bürger, in Proceedings of the 1981 International Symposium on Lepton and Photon Interactions at High Energies, edited by W. Pfeil (Bonn, 1981); W. Bartel, et al. (JADE Collaboration), DESY Report 82/023 (1982); H.J. Berend, et al. (CELLO Collaboration), DESY Report 82/021 (1982); B. Adeva, et al. (Mark J Collaboration) MIT Technical Report No. 12 (1982); C.A. Blocker, et al. (Mark II Collaboration), Phys. Rev. Lett. 49, 517 (1982).
48. I thank John Ellis for supplying me with the composite drawing (Fig. 7) of the results of the collaborations in Ref. 47.
49. See S. Olsen's discussion of toponium in the report of the e⁺e⁻ Collider Group in these proceedings.
50. See, e.g., T. Appelquist, R.M. Barnett and K. Lane, Ann. Rev. Nucl. Part. Sci. 28, 387 (1978).
51. H. Kagan, in Report of the 100 GeV Facility Subgroup of the e⁺e⁻ Collider Group, these proceedings.
52. The reader hardly needs to be reminded that one can do a much more thorough search with improved capability to detect P⁺P⁻ in all-hadron modes.
53. Note that not both neutral Higgs mesons in this decay need be more massive than $2m_t$. If both are, Z⁰ → H₁⁰H_j⁰ may be kinematically forbidden.
54. See the report of the 1 TeV Facility Subgroup of the e⁺e⁻ Collider Group for discussion of the parameters, physics capabilities and physics backgrounds of colliding linacs.
55. I thank M. Peskin for his speedy calculation of this cross section at the Summer Study. The importance of technihadron dominance in high-energy e⁺e⁻ and hadron-hadron collisions was, as far as I know, first realized in Snowmass. (See also Ref. 59.)
56. This discussion of P₈⁰' production and detection is abstracted from G. Baltay's transparencies at the Summer Study. For further details, see the report of the Hadron-Hadron Collider Group in these proceedings.
57. In his discussion, Baltay assumed the nonleptonic branching ratio of the t-quark to be 3/5. Naively, it should be 2/3, but this does not affect the results of Table 8 significantly.
58. J.A. Grifols and A. Méndez, Phys. Rev. D26, 324 (1982). These authors did not include effects of ω₈⁰ nor of scale violation in their calculations.
59. E. Eichten, private communication.
60. S. Rudaz and J. Vermaseren, CERN Preprint Th-2961 (1981).
61. J.A. Grifols and A. Méndez, Phys. Rev. D25, 253 (1982).